



# Attacking the mitochondria of colorectal carcinoma by novel 2-cyanoacrylamides linked to ethyl 1,3-diphenylpyrazole-4-carboxylates moiety as a new trend for chemotherapy



Magda F. Mohamed<sup>a,c,\*</sup>, Amna A. Saddiq<sup>d,e</sup>, Ismail A. Abdelhamid<sup>b,\*</sup>

<sup>a</sup> Department of Chemistry (Biochemistry Branch), Faculty of Science, Cairo University, Giza, Egypt

<sup>b</sup> Department of Chemistry, Faculty of Science, Cairo University, Giza, Egypt

<sup>c</sup> Department of Chemistry, Faculty of Science and Arts, Khulais, University of Jeddah, Saudi Arabia

<sup>d</sup> Department of Biology, Faculty of Science, University of Jeddah, Jeddah, Saudi Arabia

<sup>e</sup> Chair of Yousef Abdulatif Jameel of Prophetic Medicine Application, Faculty of Medicine, King Abdulaziz University, Jeddah, Saudi Arabia

## ARTICLE INFO

### Keywords:

Cyanoacrylamides linked pyrazole-4-carboxylate  
Cytotoxicity  
Molecular docking  
 $HCT_{116}$   
Apoptosis  
Morphological characterization  
Caspase-9  
Cell cycle arrest

## ABSTRACT

A novel set of 2-cyanoacrylamides linked to ethyl 1,3-diphenylpyrazole-4-carboxylates moiety were synthesized and elucidated by different spectroscopic tools. *In vitro* cytotoxic assay was carried out against different cell lines ( $Hct_{116}$ , A549, MDA-MB<sub>231</sub>, and HFB<sub>4</sub>). Ethyl 5-(2-cyano-3-(furan-2-yl)acrylamido)-1,3-diphenylpyrazole-4-carboxylate **5** achieved the potent cytotoxic effect toward all tested cancer cell lines especially colon cancer ( $HCT_{116}$ ) with  $IC_{50}$  value (30.6  $\mu$ g/ml) relative to the lead compound **3** and the standard positive control 5-FU. Additionally, it exhibited less toxic effect toward the normal human melanocytes (HFB<sub>4</sub>) cell line. Compound **5** was theoretically investigated and compared for its binding affinity to a model of protein markers relative to the lead compound **3** using two different molecular docking programs. More investigations were performed in an attempt to find out the molecular mechanism of this novel compound inside colon cancer cells, as real time PCR analysis, Elisa assay, flow cytometry, and morphological characterizations using TEM and SEM tools. Herein, we showed that compound **5** interferes with the intrinsic pathway of apoptosis at the mitochondrial level in response to an apoptogenic stimulus as cytochrome c, caspase-9 and caspases-3 which were triggered by our novel compound **5**. All molecular investigations proved that intrinsic apoptotic pathway of colorectal carcinoma was strongly initiated by the effect of compound **5** through upregulation of mitochondrial apoptosis related genes as (Caspase-3, caspase-9, BAX, P<sub>53</sub>, and cytochrome-c) and down-regulated anti-apoptotic proteins (BCL2, MMP1, CDK4, and VEGFR). Further studies proved cell cycle arrest of  $HCT_{116}$  cell lines at G2/M phase after treatment. In addition, our data revealed that our novel efficiently damage the genomic DNA of colorectal cells involving P<sub>53</sub> dependent mechanism using DPA assay. Sever morphological and ultrastructural changes were detected in colorectal cells treated by compound **5** compared to control using both scanning electron microscopy (SEM) and transmission electron microscopy (TEM).

## 1. Introduction

The great interest in the compounds containing acrylamide group is due to promising biological activities that includes anticancer [1], antimicrobial [2,3], antifungal [4], anti-inflammatory [5] and anti-diabetic [6] properties. In addition, pyrazole moiety represents an effective medicinal scaffold and exhibits a wide range of biological activities such as anti-inflammatory [7–9], anti-microbial [10,11], anti-tubercular [12,13], and anti-fungal activity [14], antidepressant activity [15], anticancer activity [16–19]. Moreover, it has been reported

that pyrazole incorporating acrylamide moiety could enhance the activity in the treatment of cancers [20–22]. Furthermore, the apoptotic mechanism is highly sophisticated, involving cascade reactions of molecular events. Up to date, all studies indicate that there are two main types of apoptotic pathways, the extrinsic and the intrinsic (mitochondrial) pathway. There was now proving that the two pathways are linked together and can influence each other [23], where each pathway need specific stimulus to begin the molecular events. Each pathway stimulates its own initiator caspase (8, 9) which, consequently, will initiate caspase-3. Caspase-3 in turn degrade the genomic DNA of

\* Corresponding authors.

E-mail addresses: [magdrafikry85@yahoo.com](mailto:magdrafikry85@yahoo.com) (M.F. Mohamed), [ismail\\_shafy@yahoo.com](mailto:ismail_shafy@yahoo.com) (I.A. Abdelhamid).

cells, degradation of most nuclear protein, cytoskeletal structure damage, appearance of apoptotic bodies and terminally, uptake through phagocytic cells [23]. The intrinsic signals that initiate cell death involve non receptor mediated stimuli that initiate the intracellular signals that directly act on targets inside the cell and trigger the mitochondrial events. Most of all stimuli rise differences in the inner membrane of mitochondrial that cause an opening (pore) in it. Then, release from the intermembrane space into the cytosol, two groups of pro-apoptotic proteins. One of these groups involves Smac/DIABLO, cytochrome *c* and the serine protease. These activate the mitochondrial pathway including caspases proteins. Where cytochrome *c* binds Apaf-1 and activate procaspase-9, forming an apoptosome and leads to activation of caspase-9 [23].

On the basis of the above assumptions and in a continuation to our research directed towards the synthesis of bioactive heterocycles [24–28], herein our studies focus on the design of new cyanoacrylamide derivatives linked to ethyl 1,3-diphenylpyrazole-4-carboxylates moiety and screening their anticancer activity against different cell lines.

## 2. Results and discussions

### 2.1. Chemistry

The starting ethyl 5-(2-cyanoacetamido)-1,3-diphenylpyrazole-4-carboxylate **3** was obtained in high % yields and purity via the direct reaction of ethyl 5-amino-1,3-diphenyl-1*H*-pyrazole-4-carboxylate **1** with 3-(3,5-dimethylpyrazol-1-yl)-3-oxopropanenitrile **2** following the literature procedures (Scheme 1) [29–32]. Knoevenagel condensation reaction of the ethyl 5-(2-cyanoacetamido)-1,3-diphenyl-1*H*-pyrazole-4-carboxylate **3** with the mole equivalent of heterocyclic-carbaldehydes **4**, namely, furan-2-carbaldehyde, thiophene-2-carbaldehyde, 1,3-diphenyl-1*H*-pyrazole-4-carbaldehyde, 3-(4-hydroxyphenyl)-1-phenyl-1*H*-pyrazole-4-carbaldehyde, 1-phenyl-3-(thiophen-2-yl)-1*H*-pyrazole-4-carbaldehyde in the presence of piperidine as a basic catalyst results in the formation of the corresponding 2-cyanoacrylamides linked to ethyl 1,3-diphenylpyrazole-4-carboxylates **5–9** (Scheme 2). The structures of the prepared compounds were elucidated based on the different spectral data. For example, the mass spectrum of compound **5** revealed molecular ion peak at *m/z* 452. <sup>1</sup>H NMR displayed a triplet signal at  $\delta$  1.03 and quartet at 4.06 ppm for the ester group. Also, it featured two singlet signals at  $\delta$  8.22 and 10.57 ppm for the yildene-H3 and NH protons respectively. In addition, the signals of the phenyl and furan protons appear as multiplets in the area of 6.88–8.16 ppm. Moreover, the <sup>13</sup>C NMR (APT) showed twenty-two different signals corresponding to 22 different carbons.

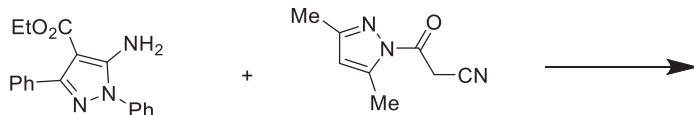
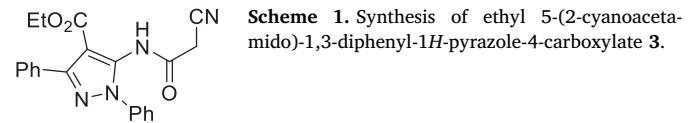
### 2.2. Cytotoxic test

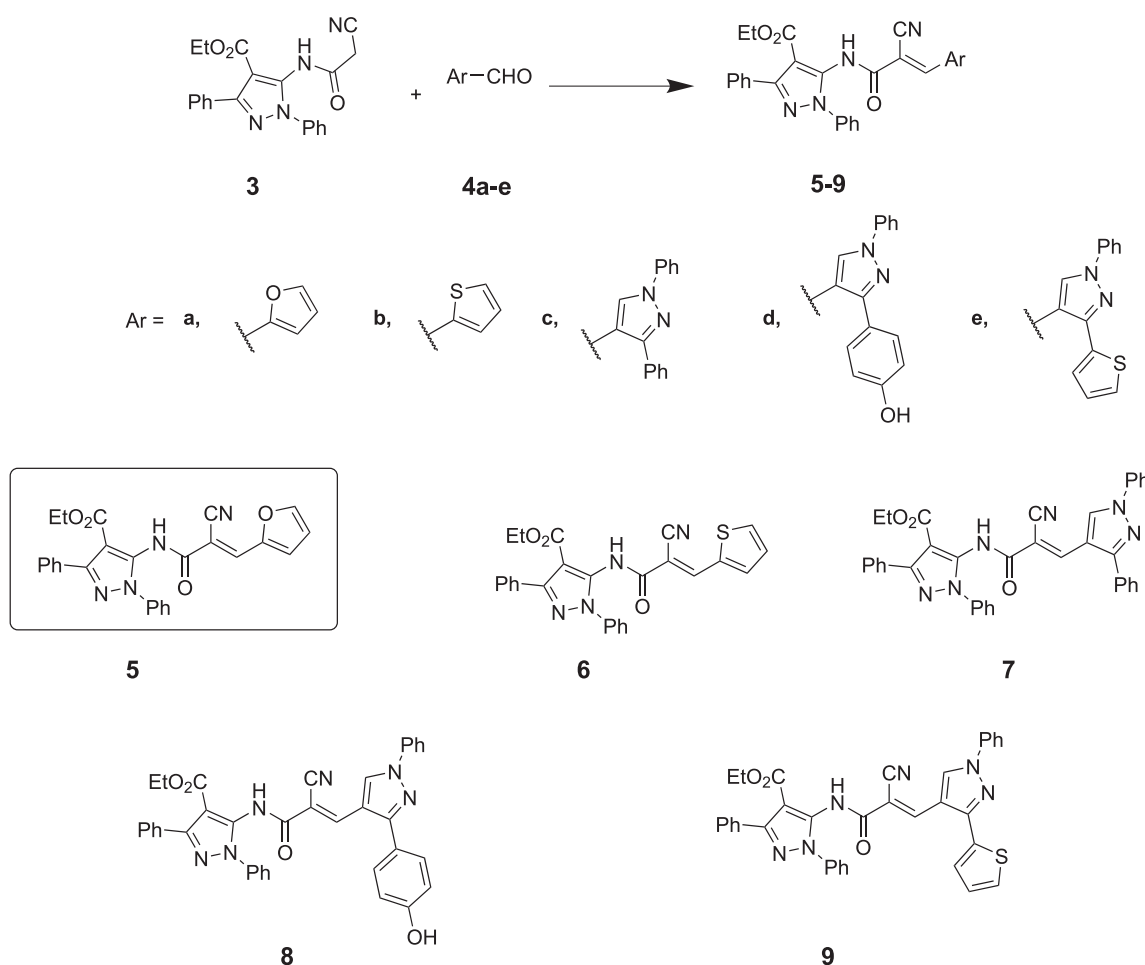
In continuation to our previous studies on cyanoacrylamide derivatives that proved noticeable cytotoxic activity [32,33], cytotoxic test was performed on a novel set of a very interesting biologically active cyanoacrylamide incorporating pyrazole moiety as illustrated in Fig. 1 and Table 1. The overall data indicated that all prepared set exposed interesting and promising cytotoxic effect toward all selected carcinoma cell lines regarding the lead compound **3**. Generally, as illustrated in Fig. 1A, compound **5** achieved the highest cytotoxic activity with IC<sub>50</sub> value (30.6 µg/ml) regarding lead compound **3** (245.3 µg/ml) and 5-FU (284.2 µg/ml) against colon cancer. Additionally, as showed in

Fig. 1A, colon carcinoma illustrated potent response (low surviving fractions) toward compounds **6** and **9** with IC<sub>50</sub> values (155.2 and 121.9 µg/ml), respectively. On the other side, compounds **7** and **8** showed less cytotoxic activity toward the same line (344.2, 348.07 µg/ml), respectively. Compound **3** (lead compound) in general show moderate activity toward colorectal cells compared to all set and potent activity relative to 5-FU. Authors referred the strong cytotoxic effect of compound **5** to the presence of additionally 2-vinylfuran group compared to the lead compound **3**. Regarding lung carcinoma, as depicted in Fig. 1B, compound **8** proved high cytotoxic effect toward this line with IC<sub>50</sub> value (96.24 µg/ml). This pronounced activity may be attributed to the presence of additional 4-(1-phenyl-4-vinyl-1*H*-pyrazol-3-yl) phenol group relative to the lead compound **3** (320. 24 µg/ml) as illustrated in Table 1. Also, this new additional group promoted and enhanced cytotoxicity much more than the positive control 5-FU (205.22 µg/ml). Also, compound **5** exhibited better cytotoxicity toward lung carcinoma cell line (200.16 µg/ml) relative to both lead and positive control compounds. In addition, compounds (**6**, **7**, and **9**) showed less cytotoxic effect (381.62, 413.81, and 446 µg/ml), respectively relative to the positive control (205.22 µg/ml). Concerning the cytotoxic effect of our novels regarding breast carcinoma (MDA-MB<sub>231</sub>), we found that all compounds (**5–9**) featured promising effects compared to the lead compound **3** (1600 µg/ml) as showed clearly in schematic diagram (Fig. 1C). It was noted that compounds (**7–9**) showed strong activity (359.27, 221.13, 375.01 µg/ml) relative to positive control (500.11 µg/ml). Compound **5** exhibited comparable activity to the positive control (approximately the same effect). In contrast, compound **6** illustrated weak cytotoxic effect with respect to 5-FU as showed in (Fig. 1C. Despite cytotoxic variations offered by our new cyanoacrylamide derivatives as promising chemotherapeutic candidate, it was necessary to check the toxic effect using normal melanocytes. Compounds **5**, which is the most active agent in this set was tested for its toxicity against HFB4 cell line. It showed less toxic effect (high surviving fractions) with inhibition concentration (1800 µg/ml) as outlined in Fig. 2. Our novel cyanoacrylamides achieved compatible effect to that recently published [31]. In contrast, previous literatures illustrated that the additional groups in cyanoacrylamide derivatives enhanced their activity much more strongly compared to that in this report regarding colon and breast carcinoma [32]. Thus, new additional pyrazole moiety into the lead cyanoacrylamide compound **3** exposed strong to moderate cytotoxic activity especially compound **5** which considered the best sensitive and selective agent toward colorectal carcinoma.

### 2.3. Computational studies

Herein protein-ligand interactions were a molecular docking or theoretically computational technique. This computational study aimed to predict the orientation, position, and most suitable binding energy of the target compound **5** when it was bound to the active site of protein. Most of Pharmaceutical research used modeling techniques for many purposes, as notably in the screening of wide spectrum of chemical reagents to select the most proper drug candidates. In the current study, the most active cytotoxic compound **5** was selected from a set of derivatives for docking study relative to the lead compound **3** in attempts to expect the mechanism of action of the target ligand. Several software applications were available, such as MOE program that calculated the geometry, and the suitable binding energy of our targets fitted into the selected active domains. In this recent study, we hope to





**Scheme 2.** Synthesis of 2-cyanoacrylamides linked to ethyl 1,3-diphenylpyrazole-4-carboxylates 5–9.

investigate the binding affinity of the most active derivative 5 against different protein markers. This study could inform us theoretically about the expected mechanistic action of this target ligand inside cancer cells. Firstly, the lead 3 and novel compound 5 were tested against selected three proteins (inhibitor of apoptosis, vascular endothelial growth factor receptor tyrosine kinase, and tubulin-colchicine-ustiloxin). The active domains of tested proteins obtained from protein database (PDB codes: bcl2-xl, 3wze, 3ut5). Authors utilized these studies in order to know if the additional 2-vinylfuran and pyrazole moieties in compound 5 affected its biological activity compared to lead compound 3. The above three domains were complexed with co-crystallized ligands (Phenyl Tetrahydroisoquinoline Amide Complex, colchicines and sorafenib) [34–36] respectively, as a standard inhibitors. The results obtained by targeting compound 5 into the active domains of the selected domains were very interesting and promising. It was observed from data outlined in Fig. 3 that compound 5 was strongly fitted into the active domains of all proteins bcl2-xl, VEGFRTK and tubulin-colchicine-ustiloxin relative to lead compound 3. The lead and target compounds (3, 5) showed different binding affinity toward them with different binding energy ( $-19.9$ ,  $-14.650$ , and  $-20.960$  Kcal/mol) relative to readings of standard ligands ( $-18.19$ ,  $-28.879$ , and  $-11.6465$  Kcal/mol) respectively. The interested binding affinities of our ligand 5 into active domains achieved through three hydrogen binding. In addition, there were several types of interactions mentioned in the dimensional representations that supported the setting of the target ligand inside the active domains. With respect to lead 3, it was bonded into the active domain 3wze by only one hydrogen bond within the amino acid (Lys A:868) and also toward 3ut5 protein within (Thr A:179). In addition to two hydrogen bonds with bcl2-xl protein through

(ASV A:102 and ARG A:105) amino acids. Regarding compound 5, it was strongly interacted into all domains by three hydrogen bonds within amino acids (ARG A:88 and GLU A:95) regarding bcl2-xl, (Asp A:1046, Glu A: 885, and lys A: 868) for 3wze domain and (Gln A:11, Ser A:140, and Ala A: 12) for 3ut5. In comparison between the target compound 5 and lead 3, It was noted that the presence of the additional 2-vinylfuran and pyrazole groups in our novel compound 5 enhanced its binding affinity toward both domains. Other interactions achieved by our compounds were carbon hydrogen bond, Pi anion, Pi cation, Pi sulfur, Pi alkyl....etc. as showed in Fig. 3. Finally, from theoretical point of view, compound 5 may follow different mechanistic pathways to inhibit cancer cells. In this report, authors suggested that compound 5 was a strong targeting agent and medical weapon to fight cancer and more molecular analysis would be done to confirm our suggestion.

#### 2.4. Real time polymerase chain reaction

Recently, we examined the expression level of the apoptosis related genes using very sensitive technical tool known as quantitative Real-Time PCR. It is used to illustrate the effect of compound 5 on different protein markers. The expression level of the following genes (BAX, P53, Caspase-9, Caspase-3, BCL2, MMP1, and CDK2) was investigated using specific primers for each gene in treated colorectal carcinoma regarding control sample and house-keeping gene (GAPDH). This cell line illustrated high sensitivity toward the potent active compound 5, in addition, compound 5 has less toxic effect toward human normal melanocytes (HFB4). Fig. 4a showed that compounds 5 strongly up-regulated the expression level of the promoter gene that trigger apoptosis (Caspase-3) (fold change = 5.335). Also, the induction level of the

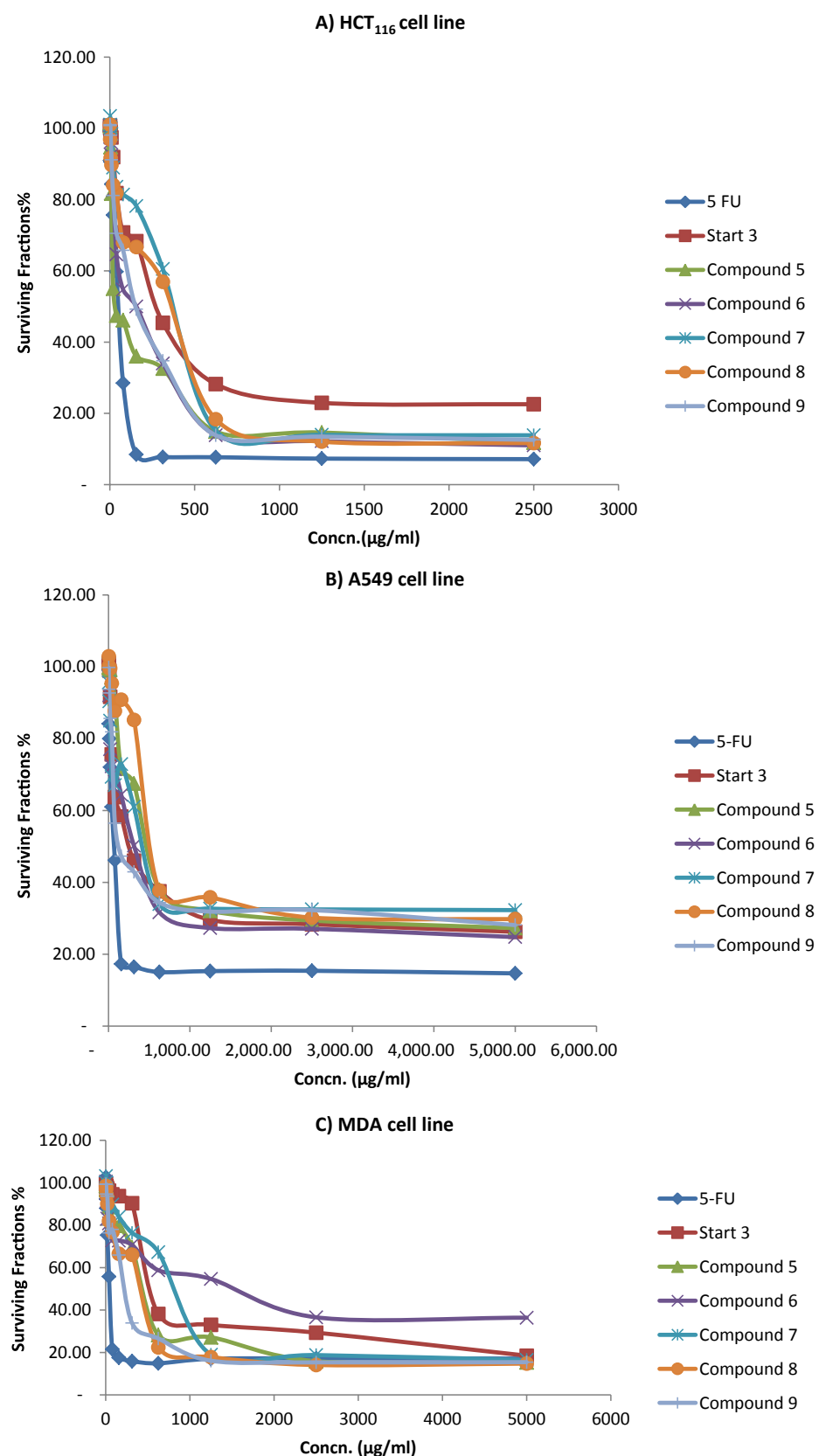


**Fig. 1.** The percent of surviving fractions of the tested start compound 3 and our novels (5–9) against different cancer cell lines (HCT116, A549, and MDA-MB231) using 5-flourouracil (5-FU) as positive control.

**Table 1**

The inhibition concentration ( $IC_{50}$ ) values of the start **3** and new compounds (**5–9**) on different human cell lines HCT<sub>116</sub>, A<sub>549</sub>, and MDA-MB<sub>231</sub> using (**5-FU**) as positive control.

Samples	$IC_{50}$ ( $\mu\text{g}/\text{ml}$ )			
	HCT <sub>116</sub>	A <sub>549</sub>	MDA-MB <sub>231</sub>	HFB <sub>4</sub>
5-FU	284.2	205.22	500.11	–
Lead compound <b>3</b>	245.3	320.24	1600	–
Compound <b>5*</b>	30.6	200.16	500.81	1800
Compound <b>6</b>	155.2	381.62	788.6	–
Compound <b>7</b>	344.2	413.81	359.27	–
Compound <b>8</b>	348.07	96.24	221.13	–
Compound <b>9</b>	121.9	446	375.01	–

suppressor gene p53 was enhanced strongly by the action of the novel compound **5** (fold change = 8.122). In addition, the two apoptotic genes BAX, and caspase-9 were up regulated efficiently with fold change values 3.660, and 3.79 respectively, by the same drug. On the other hand, compound **5** significantly down regulated the induction rate of BCL<sub>2</sub> (fold change = 0.228), CDK<sub>4</sub>(fold change = 0.442), and MMP<sub>1</sub> (fold change = 0.326) genes as depicted in Fig. 4b. Thus, enhancement the expression level of apoptotic genes P53, BAX, Caspase-9 and caspase-3, and down regulation of anti-apoptotic ones (CDK<sub>4</sub>, MMP<sub>1</sub>, and BCL<sub>2</sub>) through the treatment with our novel assumed the inhibition of cancer cells through intrinsic pathway of apoptosis.

## 2.5. DNA fragmentation

A stimulus as DNA damage, and oncogene activation, could lead to the up regulation of p53 gene. DNA breakdown may be due to the exposure to drugs or different types of radiation. Subsequently, this damage provided signals that activated the cellular kinases (ATM) and (ATR) which indicated that p53 protein was in the phosphorylated form. If the DNA damage was severe (irreversible), apoptosis was triggered [37]. Herein, our data indicated that caspase-3 was essential factor for apoptotic death stimulated by compound **5** as illustrated in PCR section. Also, this protein was necessary for DNA break down and some morphological characterizations of cell undergoing death by proteolysis and blocking many key substrates, involving the structural proteins that were necessary for keeping cell architecture [38]. In this report, colorimetric alquantization diphenylamine method was used to investigate the amount of DNA braked down from colon carcinoma treated with compound **5**. In previous studies, methods of growth measurement depend on DNA quantification, were mainly time consuming and expensive such as the Burton method [39]. In DPA method, DNA extraction steps or pretreatment steps of sample were excluded; it

outlined a major simplification of the Burton methods [33,40]. A schematic diagram is presented in Fig. 5 showed a comparison relationship between the percentages of fragmented DNA in both treated and control samples. The data here showed that compound **5** has promising effect, and it was considered as an effective agent in fragmenting cellular DNA of colorectal carcinoma. Results offered a highly percent of damage caused by our new compound **5** (24.35345%) compared to control sample (6.953224%). Thus, the efficient fragmentation of genomic DNA of colorectal carcinoma treated by the novel agent **5** makes the cell suicide.

## 2.6. Eliza assay

### a-ELISA assay for Caspase-3 protein

The best and well-known biochemical hallmark of cell death was the activation of caspases proteins. Investigation of reactive caspase-3 in cell tissues is a very important tool for apoptosis induced by many apoptotic signals. Also, sensitive and reproducible detection of active caspase-3 is mandatory to advance the explanation of cellular functions. This assay for quantifying casp-3 protein is performed according to *Human Caspase-3 (active)* kit from *invitrogen corporation* with catalog number (Catalog # KHO1091). This assay is used for the detection of active caspase-3 from lysates of human cells. Effector caspases like caspase-3 in turn cleave other proteins substrate inside the cell resulting in the apoptotic process. At least fourteen caspases have so far been implicated in human apoptotic pathway of cascades. Among these, caspase-3 was regarded to be a major protease in cell death pathway. Once it was activated, it cleaved key cellular proteins in apoptotic cells, such as the nuclear enzyme poly(ADP-ribose) polymerase (PARP), sterol regulatory element binding proteins (SREBPs), and other caspase members (caspase-2, -6, -7, and -9). “In this respect, suppression of components which act downstream of the mitochondria such as Cytochrome c and caspases can protect the cells from apoptotic insults. Accordingly, the expression levels of several anti-apoptotic proteins have been shown to correlate with colon carcinoma susceptibility to chemotherapy” [41]. Data measurements indicated that caspase-3 protein was strongly induced by the effect of our target compound **5** to reach (338.1) relative to control sample (17.27). This was illustrated in Table 2 and Fig. 6a in which the expression level of caspase-3 protein was increased approximately 20-fold compared to that of negative control.

### b-ELISA assay for cytochrome-c protein

First, Cytochrome c was identified and quantified according to the manuscript instructions followed in cytochrome-c human elisa kit (ab119521 from abcam). It was a component required for cell death and caspase-3 up-regulation. Now, challenge was directed for discovering a new agent that target cancer cell and overcome its resistance

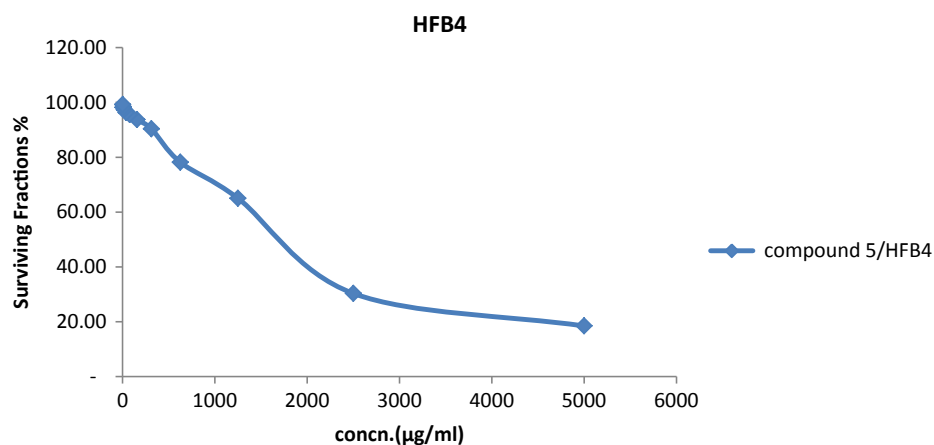


Fig. 2. Viability percent of the most active derivative **5** against the normal melanocytes (HFB4) using prism software program.

tools (anti-apoptotic strategies). So, targeting the mitochondria as a novel strategy for cancer therapy has taken author attention where in this regard, anticancer agents **5** can target some pathways of the mitochondria that may converge onto the intrinsic death pathway [42]. Although, the deregulation of some proteins as HIF, and c-MYC lead to high resistance of cancer cell. Direct attacking mitochondria may enable us to beat on the resistance problem [43]. Mitochondria were the main energy source for the cell and carcinoma cells displayed higher energy request for survival; so, targeting it appeared to be an attractive tool. This could be illustrated through the role of mitochondria in resisting several death factors within the release of some critical apoptotic proteins such as cytochrom-c (cyt c), Apaf-1, and Smac/DIABLO, which exist normally in the inter-membrane region. Thus, these have made

mitochondria more interested and favorable target for therapeutic manipulation. The overall measurement results were summarized in (Table 2) which indicated that compound **5** was an effective agent that clearly increased the protein level percent of cytochrome-c to reach (0.603) relative to controls (0.031) respectively. Also, this data was outlined diagrammatically in Fig. 6b which referred to the potency of compound **5** in increasing the apoptotic protein (cyt c).

#### c- ELISA assay for VEGF-A protein

Previous literatures illustrated that vascular endothelial growth factor (VEGF) is a prevailing angiogenic agent that plays a critical role in the progress and spread of colon cancer [44]. Although improvements and advances in treatment tools, the percent of mortality still high, with current transition into the liver in approximately 50% of

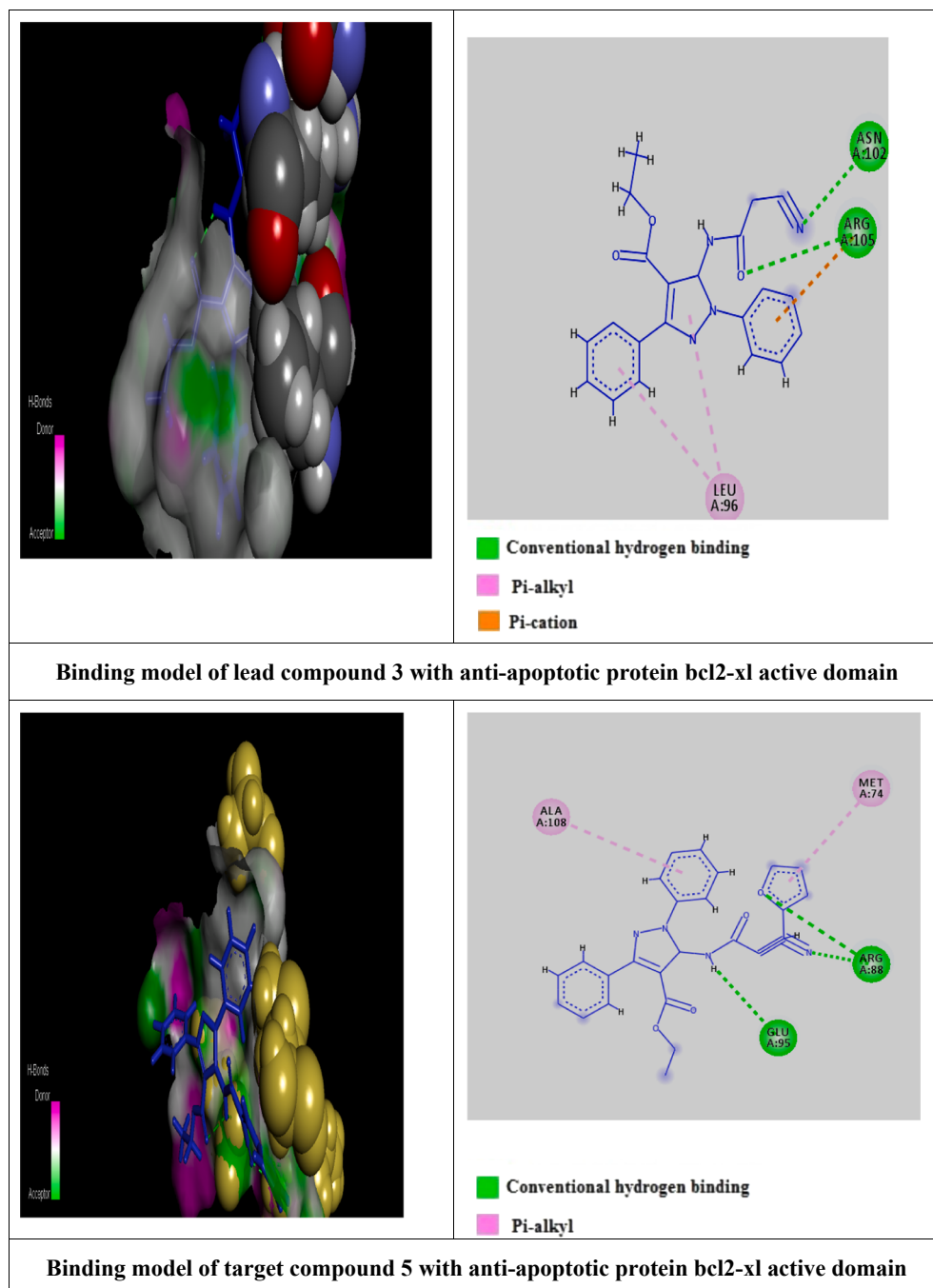


**Fig. 3.** Computational studies involved 2D and 3D dimensional representations showed promising binding affinities of the novel compound **5** relative to the lead compound **3** against the three active binding sites (**bcl2-xL**, **3wze**, and **3ut5**) respectively.

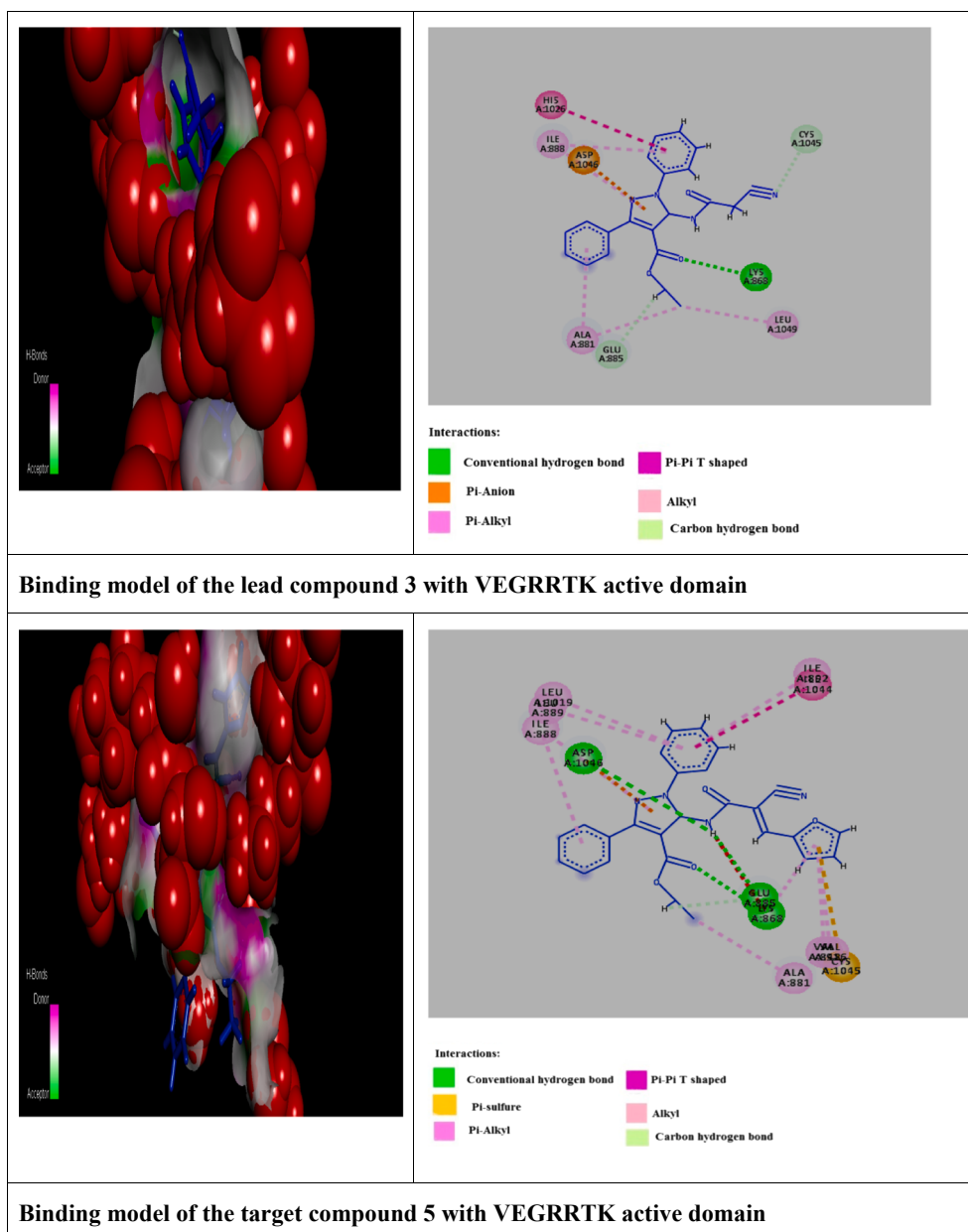


Fig. 3. (continued)

patients [44]. Also, it is previously demonstrated that overexpression of tumor (VEGF) is correlated to tumor advanced stage or invasion in different types of common human cancer. Its overexpression in colorectal carcinoma tissue shows poor prediction, although paradoxically data in some studies showed that (VEGF) has no significant value in colorectal tissue. VEGF-A protein is the most widely angiogenic protein studied, it increases permeability and vascularization of blood vessels. In this assay, we estimated the expression value of VEGF-A in colon cells treated with our new inhibitor for 48 h of treatment. Measurements outlined in both (Table 2 and Fig. 6a) show low expression level of antiapoptotic protein (VEGF) due to the cytotoxic effect of compound 5 to reach (480.6Pg/ml) in comparison to control sample (1487Pg/ml).

It was concluded from Elisa assay that, compound 5 was a very potent chemotherapeutic drug which significantly promoted the up regulation level of caspase-3, and cytochrome-c proteins and down regulated the anti-apoptotic (VEGF-A) protein efficiently as showed in (Fig. 6a, b).

## 2.7. Analysis using TEM and SEM

Cell death physiologically occurs primarily via conserved form of suicide cells known apoptosis, which may be induced by several factors as chemotherapeutic chemicals, cytokines, or loss of some growth factors. Apoptosis was well characterized morphologically by severe disruption in cell shape such as cell shrinkage and disintegration of cells contact. In cancerous cells, sever fragmentations, apoptotic nuclei and signs of phagocytosis have been observed. Also, the morphological characteristics were small apoptotic bodies with small fragments of chromatin (nuclear condensation and budding) were used to quantify an apoptotic index [45]. In this study, we investigated apoptotic cell death of colon cancer treated with cytotoxic agent (compound 5) by TEM. "Since apoptosis is characterized by specific morphological features, it can be detected by specifically identifies DNA fragmented into nucleosome units, a characteristic of apoptosis. Nuclei of the central cells were fragmented, indicating that these cells were apoptotic. Drug-treated HCT116 cells have shown significant morphological changes

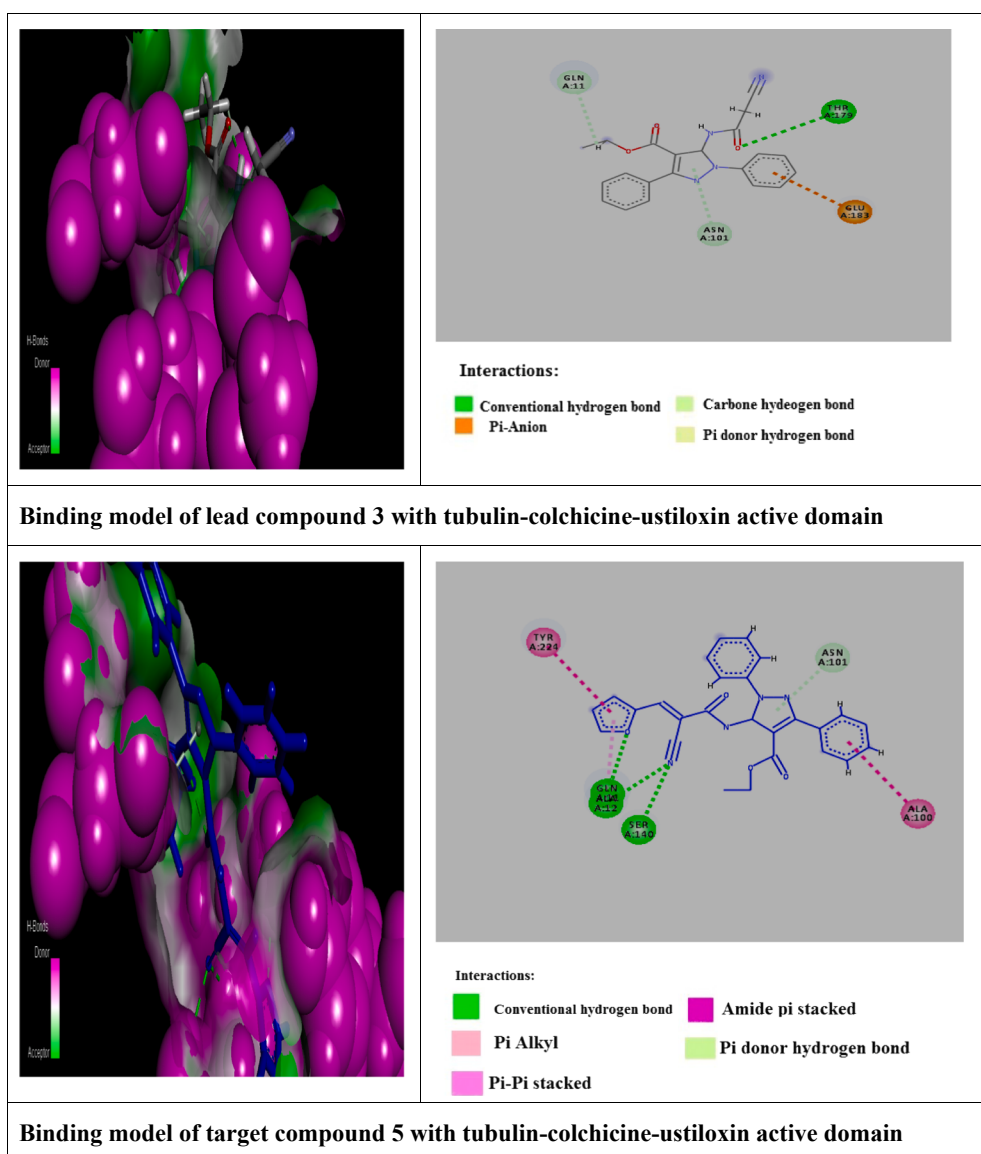


Fig. 3. (continued)

which include small group of shrunken and retracted cells from substratum". Before treatment, cells appeared in Fig. 7a with their normal and homogenous form with simple cytoplasmic organization. Also, organelles, nucleolus and mitochondria showed normal pattern. Few numbers of mitochondria appeared with their elongated structures. After 48 h of compound 5 treatment, HCT116 cells acquired many different features as showed clearly in Fig. 7b, c, and d. Treated cells showed many signs of apoptotic death as increased cell granularity, nuclear change and nuclear condensation included (Karyolysis, Pyknosis, and Karyorrhexis). In addition, detachment from the surrounding cells in the same tissue occurred, membrane blabbing, appearance of many apoptotic bodies, change in shape and structures of mitochondria. At the end, all these data obtained by TEM tool indicated that colorectal cells treated with our new drug showed phenomena of early and late stages of apoptosis. Regarding SEM analysis, it was a technique utilized by many researchers for evaluating and analysis of healthy and tumor cells. It provides enough information to analyze the surface and morphology of the cancer cell. The study aimed to check and analyze the morphology of HCT<sub>116</sub> cells only and drug 5 treated HCT cells. From the SEM image obtained (Fig. 8a), the control HCT<sub>116</sub> cells showed flat and highly dynamic cells, with filopodia and lamellipodia. In contrast, the treated cells (Fig. 8b) demonstrate shrunken

morphology, irregular distribution of cytoplasm small ruffles, intermittent parts of cancer cell, loss of membrane extensions and detached from substratum. In addition, increasing average of cell roughness and cell diameter were clearly indicated in the figure below. Fig. 8 indicated that image dimensions (X, Y, and D) for both control and treated samples were (57.9, 48.4, and 75.5  $\mu\text{m}$ ) and (66.3, 41.1, and 78  $\mu\text{m}$ ), respectively. These dimensions reading above photos proved that cellular swelling or cloudy swelling may occur due to cellular hypoxia caused by our novel agent 5, which damaged the cell membrane pump. The cellular swelling was the first manifestation of almost all forms of injury to cells. In addition, green readings illustrated the diameter of randomly selected pores for both control and tested sample which also indicated that compound 5 cause severe damage to the colorectal carcinoma (HCT<sub>116</sub>) cell line. Finally, different microscopic techniques utilized in this section suggested that our novel compound 5 could be a promising and an effective choice for treatment of colorectal carcinoma.

#### 2.8. Flow cytometry assay

This assay was performed using flow cytometry investigation after 48hrs of treatment using (30.6  $\mu\text{g/ml}$ ) of compound 5 with colorectal

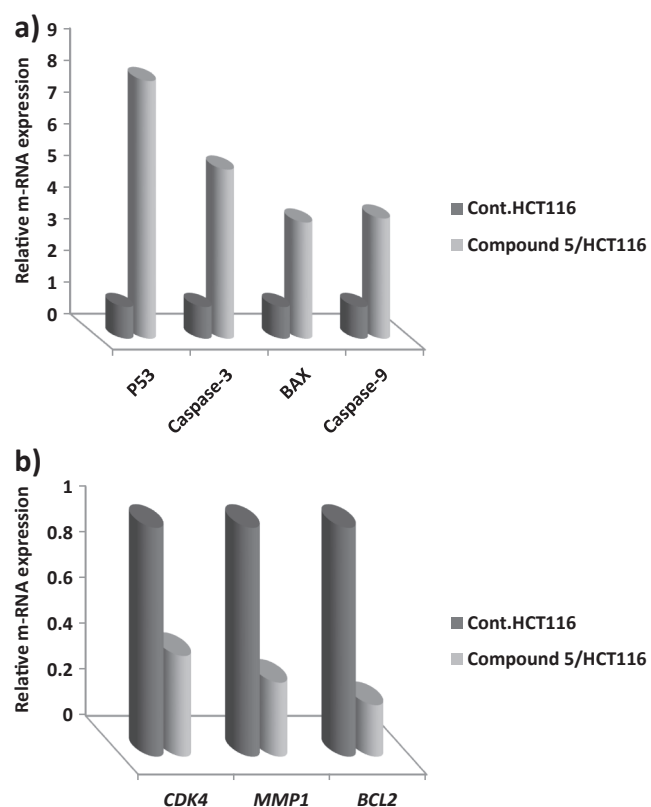


**Fig. 4.** Relative m-RNA expression diagrams of apoptotic proteins and anti-apoptotic protein for colorectal carcinoma treated with compound 5, versus control using real time PCR technique.

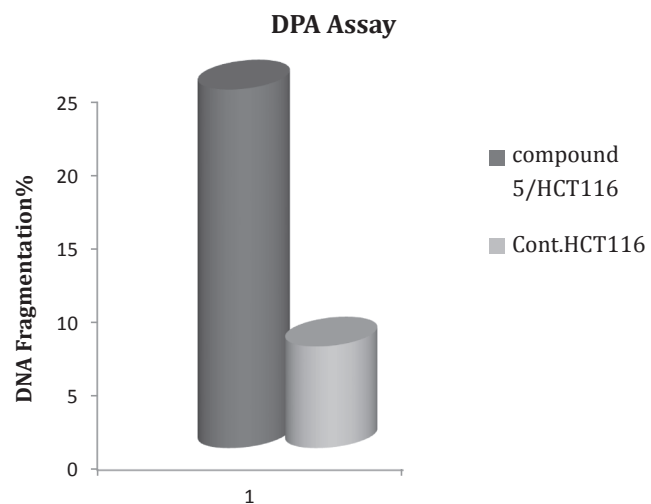


**Fig. 5.** Diagram outlined colorimetric DPA assay of HCT116 cells treated with novel compound 5 for 48 hrs of treatment at 37 °C and its control.

**Table 2**

Eliza assay for VEGF, Caspase 3, and Cytochrome-c proteins in (HCT116) cell line exposed to compound 7 for 48 h of treatment.

Samples	Caspase-3		Cytochrome-c		VEGF	
	Pg/ml	fld	Pg/ml	fld	Pg/ml	fld
Cont.HepG2	17.27	1	0.03053	1	1487	1
Compound 5/HepG2	338.1	19.5773	0.603	19.75	840.6	0.565

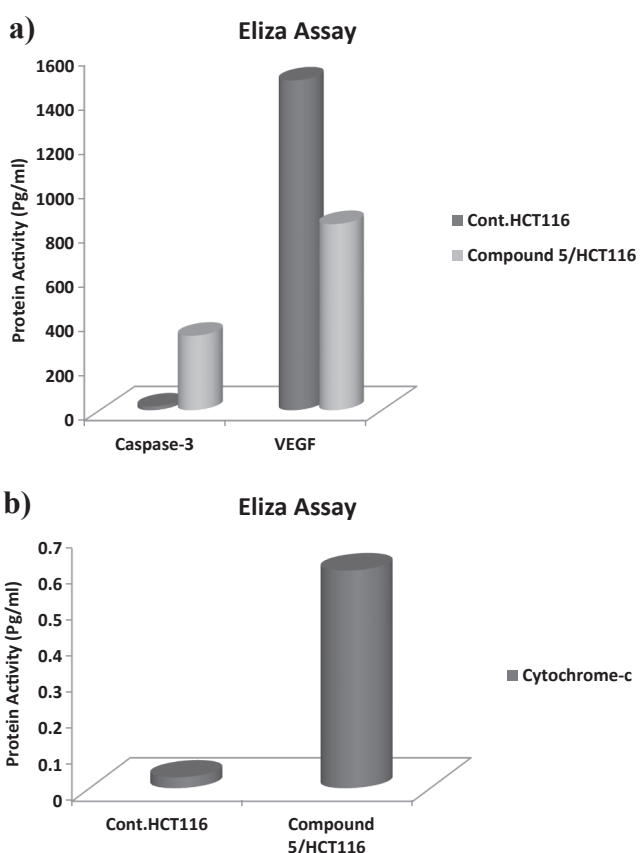


**Fig. 6.** Diagrams outlined the effect of compound 5 on proteins activity of a) Caspase 3, and VEGFR. B) Cytochrome-c, against colorectal carcinoma.

carcinoma cell line (HCT116). All data was recorded in [Table 3](#) and outlined in [Fig. 9](#). Our previous literature [32] illustrated that cyanoacrylamide derivatives proved a critical role on apoptosis pathway as a cytotoxic agents. Also, most of these derivatives exhibited effective cell death on other cell lines as breast carcinoma regarding different mechanistic pathway. Compound 5 was among the new prepared set, which selected for further molecular studies due to its potent cytotoxic effect regarding colon cancer. As illustrated in [Table 3](#), the percentage of apoptosis increased approximately by 14-fold (16.26%) relative to control sample (1.84%). Early apoptosis achieved (5.73%) regarding the control (0.92%) and the percentage of late apoptosis reached (8.04%) with respect to control (0.5%). Also, it was clearly observed that, there was a significant increase in the percentage of necrotic cells for treated sample (2.49%) compared to untreated cells (0.42%). With respect to cell cycle assay, DNA loss was considered as a part of apoptosis fraction which resulted in sub-G1 peak which can be investigated by flow cytometry technique. Quantitative determination of the amount of PI intercalated to (DNA) was used as indicator to know cell cycle distribution phases. To find mechanism of apoptosis mediated by compound 5 treatment, cell cycle analysis was performed to check out sub-G1 peak changes. This promising new target induced cell cycle arrest at G2/M phase in which all most of cell populations accumulated in this phase (29.45%) regarding control sample (4.82%). This arrest was at the expense of cell distribution on both G1 and S phases as showed in [Fig. 9](#). Authors in this report suggested that this arrest at G2/M phase may be induced by deactivation of some transcriptional factors that were responsible for division, including cyclin and CDC proteins [46]. In addition, this may be due to protein down-regulation which responsible for cell cycle progression at G2/M phase.

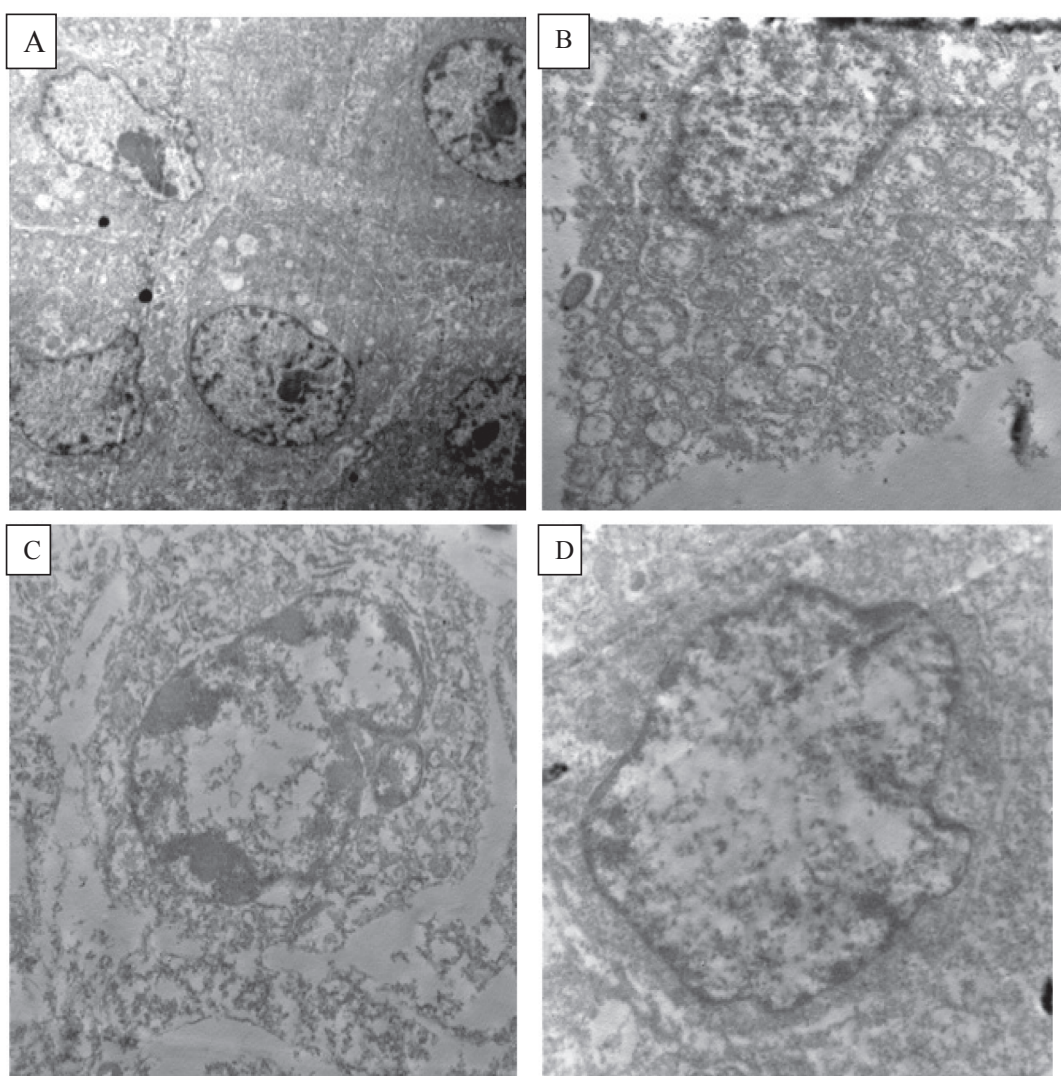


**Fig. 7.** Microscopic examinations for colorectal cells treated with novel **5** using (TEM) technique for 48 hrs of incubation. (a) Normal pattern of control cells at magnification powers (3000x). (b, c, and d) HCT116 cells treated with  $IC_{50}$  of compound **5**, at different three magnification powers (12000x, 15000x and 12000x) respectively.

### Conclusion

Apoptosis was considered as a regulated process, identified by certain morphological and biochemical characterizations in which activation of caspases played a critical role. In apoptotic pathways, different key apoptotic proteins have been identified to be upregulated or downregulated. However, mechanisms of (activation/inactivation) of these proteins were not fully understood. The significance of understanding the mechanistic machinery that control programmed cell death, being initiated by various chemotherapeutic agents was very critical and attracts the attention of researchers in this area. There was an evident to suggest a new promising chemotherapeutic cyanoacrylamide compound **5** that showed high cytotoxic activity toward colorectal carcinoma. Authors performed different theoretical and molecular experiments in attempts to explore the mechanism of action of compound **5**. Theoretically, compound **5** exerted its mechanistic action to inhibit carcinoma through its high binding affinity to the tested protein markers. Compound **5** was strongly fitted into the active domains (bcl2-xL, 3wze, 3ut5) through 3 hydrogen binding compared to the lead compound **3**. It was suggested that the presence of additional 2-cyanoacrylamides linked to ethyl 1,3-diphenylpyrazole-4-carboxylates group in compound **5** was responsible for this enhancement in activity.

Induction of apoptosis by compound **5** in colon carcinoma cell line was evaluated by different molecular and morphological characteristics. Molecular assessment outlined that compound **5** exposed its cytotoxic activity against colorectal carcinoma through upregulation of genes related to intrinsic pathway of apoptosis as (Caspase-3, caspase-9, BAX, and cytochrome-c). Finally, we can conclude that compound **5** exert its cytotoxic action theoretically through different mechanisms, as induction of apoptosis (by blocking anti-apoptotic proteins), inhibiting microtubule which are required for cell division, and inhibiting kinases' activity. In addition, further molecular studies illustrated that it inhibited colorectal carcinoma through the induction of the mitochondrial apoptotic pathway.

### 3. Experimental

#### 3.1. Materials and method

##### 3.1.1. Chemistry

"Melting points were determined on a Stuart melting point apparatus and are uncorrected. The IR spectra were measured as KBr pellets on a FTIR Bruker-Vector 22 spectrophotometer.  $^1H$  and  $^{13}C$  NMR spectra were measured using Bruker Ultrashield 400 MHz or Ascend

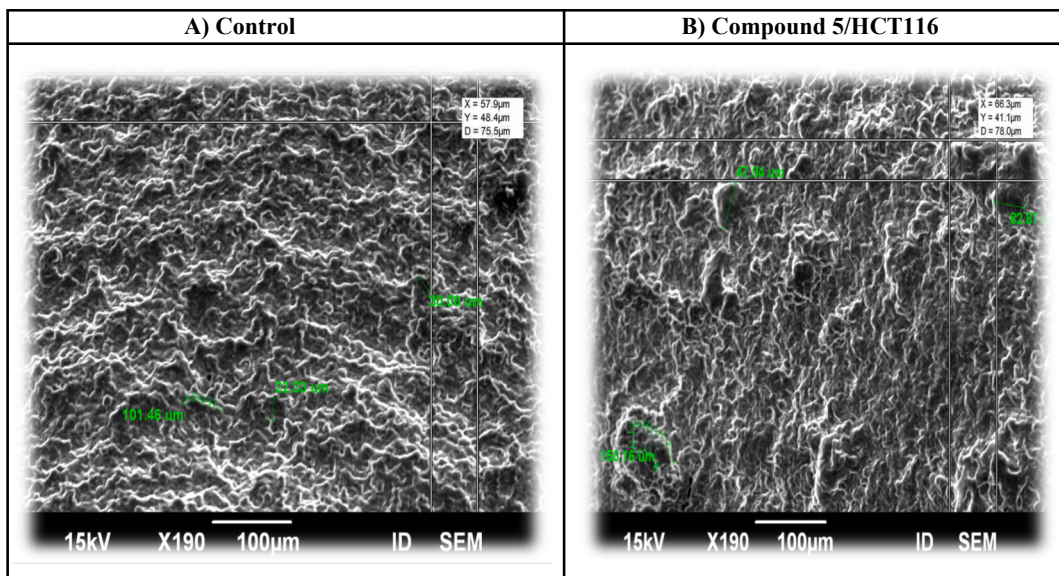


**Fig. 8.** Scanning electron microscope (SEM) images in 3D dimensions, showing apoptotic effect of compound 5 (30.6  $\mu$ g/ml) on cell surface disruption. (A) Untreated colon carcinoma. (B) Colon cells treated with compound 5 for 48 h treatment.

**Table 3**  
Apoptosis and cell cycle assay of compound 5/HCT116 in relation to the control samples.

Samples	Flow cytometer analysis			
	G0/G1 %	S %	G2/M %	Apoptosis %
Compound 5/HCT116	37.61	32.94	29.45	16.26
Control HCT116	58.14	37.04	4.82	1.84

400 MHz ( $^1\text{H}$ : 400 MHz,  $^{13}\text{C}$ : 100.6 MHz) instruments using TMS as internal standard. Mass spectra were measured on a Shimadzu GCMS-Q-1000 EX mass spectrometer at 70 eV. The elemental analyses were carried out at the Microanalytical Center, Cairo University using Automated analyzer CHNS, Vario EL III, Elemental, Germany”

**Ethyl 5-(2-cyanoacetamido)-1,3-diphenyl-1*H*-pyrazole-4-carboxylate (3)**

Ethyl 5-amino-1,3-diphenyl-1*H*-pyrazole-4-carboxylate (10 mmol) 1 was added to 3-(3,5-dimethyl-1*H*-pyrazol-1-yl)-3-oxopropanenitrile 2 (10 mmol) in dry toluene (20 mL). The mixture was heated at reflux for 3 h. The solvent was evaporated and crude product was purified by crystallization from ethanol to give yellow crystals (88%), mp 166–168 °C, IR (KBr):  $\nu$  3406, 3253, 3182 (NH), 2261 (CN), 1748 (COO), 1677 (CONH)  $\text{cm}^{-1}$ ,  $^1\text{H}$  NMR (400 MHz, DMSO- $d_6$ ):  $\delta$  1.03 (t, 3H,  $^3J$  7.2 Hz,  $\text{CH}_3\text{CH}_2$ ), 3.99 (s, 2H,  $\text{CH}_2$ ), 4.02 (q, 2H,  $^3J$  7.2 Hz,  $\text{CH}_3\text{CH}_2$ ), 7.21–7.39 (m, 10H, ArH), 10.42 (br s, 1H, NH) ppm,  $^{13}\text{C}$  NMR (100 MHz, DMSO- $d_6$ ):  $\delta$  13.6 ( $\text{CH}_3\text{CH}_2$ ), 25.9 (COCH<sub>2</sub>), 59.7 ( $\text{CH}_3\text{CH}_2$ ), 115.5, 125.5, 127.9, 128.1, 128.5 (CN), 128.9, 129.1, 130.3, 138.5, 145.4, 145.5, 161.8 (COO), 161.9 (CONH) ppm, MS (EI, 70 eV):  $m/z$  374 [M]<sup>+</sup>, Anal. Calcd. for C<sub>21</sub>H<sub>18</sub>N<sub>4</sub>O<sub>3</sub>: C, 67.37; H, 4.85; N, 14.96. Found: C, 67.19; H, 4.63; N, 14.68.

**Ethyl 5-(2-cyano-3-(furan-2-yl)acrylamido)-1,3-diphenyl-1*H*-pyrazole-4-carboxylate (5)**

Pale yellow crystals (79%). Mp: 254–258 °C. IR (KBr):  $\nu_{\text{max}}$ /cm<sup>-1</sup> 3295 (NH), 2261 (CN), 1692 (CO).  $^1\text{H}$  NMR (400 MHz, DMSO- $d_6$ ):  $\delta$  1.03 (t, 3H,  $^3J$  = 7.1 Hz,  $\text{CH}_3\text{CH}_2$ ), 4.06 (q, 2H,  $^3J$  = 7.1 Hz,  $\text{CH}_3\text{CH}_2$ ), 6.88 (m, 1H, furan-H), 7.26 (m, 1H, furan-H), 7.31–7.51 (m, 10H, Ar-H), 8.16 (d, 1H, furan-H), 8.22 (s, 1H, vinyl-H), 10.57 (s, 1H, NH).  $^{13}\text{C}$  NMR (DMSO- $d_6$ ):  $\delta$  14.2, 60.4, 100.7, 106.3, 114.7, 116.2, 116.4, 123.6, 126.2, 128.5, 128.8, 128.9, 129.4, 129.7, 130.9, 137.4, 138.9, 144.3, 145.9, 146.9, 148.7, 149.9, 160.1. MS (EI,

70 eV): 452 [M]<sup>+</sup>, Anal. Calcd. for C<sub>26</sub>H<sub>20</sub>N<sub>4</sub>O<sub>4</sub>: C, 69.02; H, 4.46; N, 12.38. Found: C, 69.14; H, 4.32; N, 12.51.

**Ethyl 5-(2-cyano-3-(thiophen-2-yl)acrylamido)-1,3-diphenyl-1*H*-pyrazole-4-carboxylate (6)**

Pale yellow crystals (78%). Mp: 226–228 °C. IR (KBr):  $\nu_{\text{max}}$ /cm<sup>-1</sup> 3294 (NH), 2260 (CN), 1690 (CO).  $^1\text{H}$  NMR (400 MHz, DMSO- $d_6$ ):  $\delta$  1.12 (t, 3H,  $^3J$  = 7.1 Hz,  $\text{CH}_3\text{CH}_2$ ), 4.04 (q, 2H,  $^3J$  = 7.1 Hz,  $\text{CH}_3\text{CH}_2$ ), 7.23–7.39 (m, 11H, Ar-H and thiophene-H), 7.99 (d, 1H, thiophene-H), 8.18 (d, 1H, thiophene-H), 8.60 (s, 1H, vinyl-H), 10.57 (s, 1H, NH).  $^{13}\text{C}$  NMR (DMSO- $d_6$ ):  $\delta$  14.2, 60.3, 101.6, 106.6, 116.7, 126.2, 128.4, 128.8, 128.9, 129.3, 129.5, 129.7, 130.9, 136.2, 136.5, 139.0, 139.4, 145.4, 145.9, 146.8, 160.4, 162.7. MS (EI, 70 eV): 468 [M]<sup>+</sup>, Anal. Calcd. for C<sub>26</sub>H<sub>20</sub>N<sub>4</sub>O<sub>3</sub>S: C, 66.65; H, 4.30; N, 11.96. Found: C, 66.78; H, 4.62; N, 12.12.

**Ethyl 5-(2-cyano-3-(1,3-diphenyl-1*H*-pyrazol-4-yl)acrylamido)-1,3-diphenyl-1*H*-pyrazole-4-carboxylate (7)**

Pale yellow crystals (78%). Mp: 280–282 °C. IR (KBr):  $\nu_{\text{max}}$ /cm<sup>-1</sup> 3310 (NH), 2261 (CN), 1690 (CO).  $^1\text{H}$  NMR (400 MHz, DMSO- $d_6$ ):  $\delta$  1.01 (t, 3H,  $^3J$  = 7.1 Hz,  $\text{CH}_3\text{CH}_2$ ), 4.05 (q, 2H,  $^3J$  = 7.1 Hz,  $\text{CH}_3\text{CH}_2$ ), 7.22–7.71 (m, 18H, Ar-H), 7.98 (d, 2H, Ar-H), 8.22 (s, 1H, vinyl-H), 9.25 (s, 1H, pyrazole-H5), 10.69 (s, 1H, NH).  $^{13}\text{C}$  NMR (DMSO- $d_6$ ):  $\delta$  14.2, 16.3, 104.3, 106.7, 114.9, 116.9, 120.2, 126.2, 128.4, 128.5, 128.8, 128.9, 129.4, 129.45, 129.5, 129.7, 129.8, 129.9, 130.4, 130.9, 131.3, 138.9, 139.1, 143.2, 145.9, 146.8, 155.3, 160.5, 162.7. MS (EI, 70 eV): 604 [M]<sup>+</sup>, Anal. Calcd. for C<sub>37</sub>H<sub>28</sub>N<sub>6</sub>O<sub>3</sub>: C, 73.50; H, 4.67; N, 13.90. Found: C, 73.63; H, 4.51; N, 13.72.

**Ethyl 5-(2-cyano-3-(3-(4-hydroxyphenyl)-1-phenyl-1*H*-pyrazol-4-yl)acrylamido)-1,3-diphenyl-1*H*-pyrazole-4-carboxylate (8)**

Pale yellow crystals (76%). Mp: 272–274 °C. IR (KBr):  $\nu_{\text{max}}$ /cm<sup>-1</sup> 3292 (NH), 2260 (CN), 1690 (CO).  $^1\text{H}$  NMR (400 MHz, DMSO- $d_6$ ):  $\delta$  1.01 (t, 3H,  $^3J$  = 7.1 Hz,  $\text{CH}_3\text{CH}_2$ ), 4.03 (q, 2H,  $^3J$  = 7.1 Hz,  $\text{CH}_3\text{CH}_2$ ), 6.97 (d, 2H, Ar-H,  $J$  = 8.1 Hz), 7.22–7.63 (m, 17H, Ar-H), 7.95 (d, 2H, Ar-H,  $J$  = 8.1 Hz), 8.20 (s, 1H, vinyl-H), 9.19 (s, 1H, pyrazole-H5), 9.92 (s, 1H, OH), 10.63 (s, 1H, NH).  $^{13}\text{C}$  NMR (DMSO- $d_6$ ):  $\delta$  14.2, 16.3, 103.6, 106.6, 114.7, 116.3, 117.1, 119.6, 120.1, 121.9, 126.1, 128.4, 128.8, 128.9, 129.4, 129.7, 130.3, 130.7, 130.9, 138.9, 139.1, 139.4, 143.6, 145.9, 146.9, 155.6, 159.1, 160.6, 162.7. MS (EI, 70 eV): 620 [M]<sup>+</sup>, Anal. Calcd. for C<sub>37</sub>H<sub>28</sub>N<sub>6</sub>O<sub>4</sub>: C, 71.60; H, 4.55; N, 13.54. Found: C, 71.48; H, 4.41; N, 13.71.

**Ethyl 5-(2-cyano-3-(1-phenyl-3-(thiophen-2-yl)-1*H*-pyrazol-4-yl)acrylamido)-1,3-diphenyl-1*H*-pyrazole-4-carboxylate(9)**

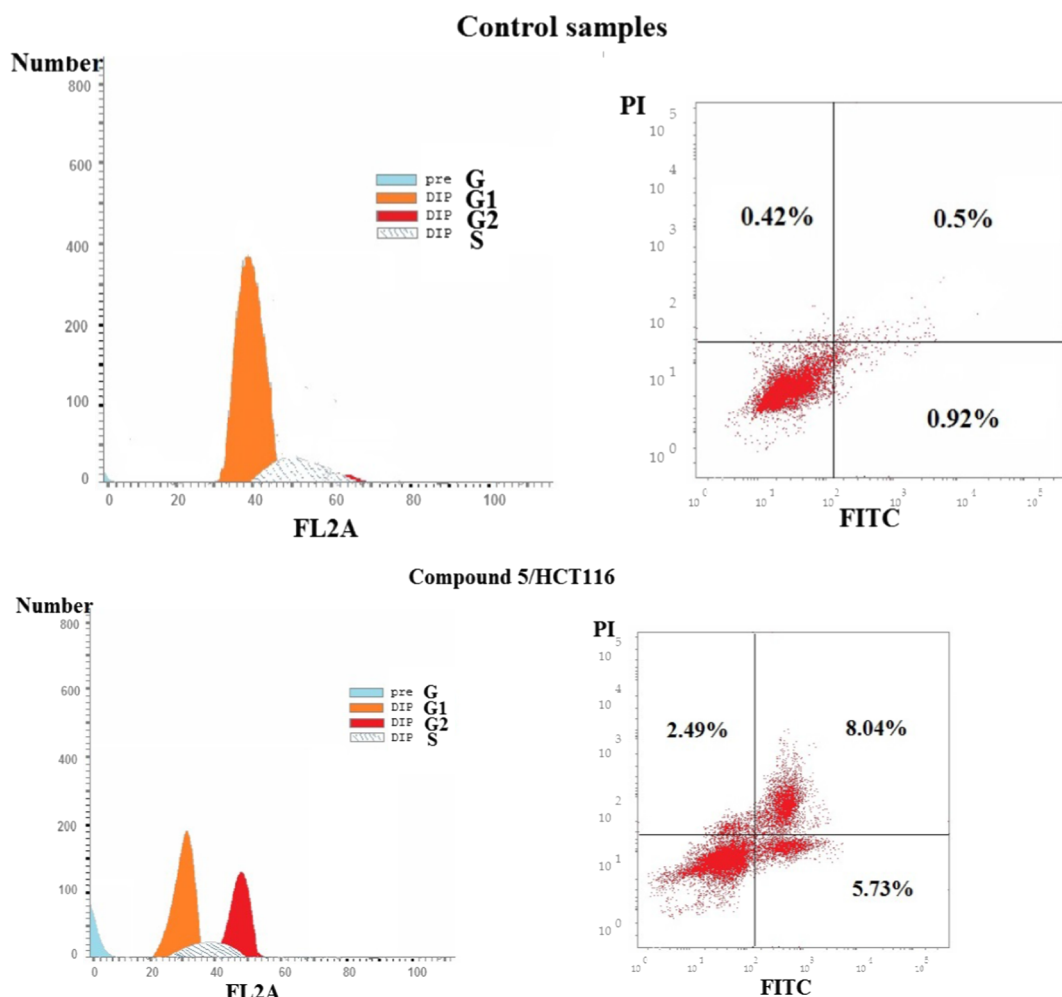


**Fig. 9.** DNA histograms of cell cycle analysis and the percent of apoptosis of HCT116 cells after 48 h of treatment with compound 5. The percentage and distribution of cells in each phase of the cell cycles were illustrated.

Pale yellow crystals (70%). Mp: 248–250 °C. IR (KBr):  $\nu_{\text{max}}/\text{cm}^{-1}$  3305 (NH), 2261 (CN), 1689 (CO). <sup>1</sup>H NMR (400 MHz, DMSO-*d*<sub>6</sub>): δ 1.0 (t, 3H, <sup>3</sup>J = 7.1 Hz, CH<sub>3</sub>CH<sub>2</sub>), 4.06 (q, 2H, <sup>3</sup>J = 7.1 Hz, CH<sub>3</sub>CH<sub>2</sub>), 7.24–7.95 (m, 18H, Ar-H and thiophen-H), 8.39 (s, 1H, vinyl-H), 9.24 (s, 1H, pyrazole-H5), 10.73 (s, 1H, NH). <sup>13</sup>C NMR (DMSO-*d*<sub>6</sub>): δ 14.2, 60.3, 104.9, 106.9, 114.6, 116.8, 119.6, 120.1, 126.1, 128.4, 128.6, 128.7, 128.8, 128.9, 129.0, 129.4, 129.7, 130.3, 130.4, 130.9, 132.6, 138.8, 138.9, 142.4, 145.9, 146.8, 149.2, 160.6, 162.6. MS (EI, 70 eV): 610 [M<sup>+</sup>]. Anal. Calcd. for C<sub>35</sub>H<sub>26</sub>N<sub>6</sub>O<sub>3</sub>S: C, 68.84; H, 4.29; N, 13.76. Found: C, 68.71; H, 4.43; N, 13.91.

### 3.2. MTT assay

We started after preparation of our novel series by investigating their cytotoxic activity against different cancer cell lines as A<sub>549</sub>, HCT<sub>116</sub>, and MDA-MB<sub>231</sub>. In addition, only compound 5 was selected and tested against normal human skin melanocytes cell line (HFB4) for 48 h of treatment using MTT analysis. All cell lines were purchased from American Tissue Culture Collection (Rockville, MD, USA), and cultured at 37°C with 5% carbonic acid gas in an exceedingly humidified atmosphere in RPMI-1640 media supplemented with 10% fetal bovine serum. All the measurements were carried out according to the recently published literature [47]. 5-flourouracil (5-FU) was a commercial anticancer drug, utilized as positive control in this assay. In addition, negative cell culture control was included, and the solvent used was DMSO to prepare 5 mg/ml as stock solution form each compound. All stock solutions prepared were filtered via 0.22 mL

syringe filter. Double fold dilutions were prepared from stock ones using freshculture media(RPMI-1640). After incubation period, residual living cells were exposed to 50 µl of filtered MTT (5 mg/ml) for 4 h. MTT was eliminated and plates were washed several times with PBS. ELISA plate reader was used to determine the optical densities at 570 nm. Surviving fractions were investigated and calculated. The IC<sub>50</sub> values of all derivatives including 5-FU were determined using the prism program.

### 3.3. Molecular docking studies

This was a simulation assay utilized here in an attempt to theoretically discover the mechanistic pathways of our novel synthesized compound 5 against different protein markers, before starting our experimental session to save time and money. The two docking programs used were MOE and BIOVIA Discovery Studio programs. The first program helps us to check the binding affinity of compound 5 toward the active sites of set proteins as ((inhibitor of apoptosis, tubulin-colchicine-ustiloxin, and vascular endothelial growth factor receptor tyrosin kinase,)). In which standard ligand complexed with these proteins were removed and replaced by our target agent after selecting the suitable binding energy. The second one was used at the end to visualize all binding in 3D and 2D dimensions regarding all types of interactions recorded between compound 5 and active domains of the tested protein set. All measurements were carried out in details according to our previous literatures [32,47]. Where our protein set were downloaded from protein database ([www.RCSB.org](http://www.RCSB.org)) in complex with standard co-

**Table 4**

Sense and antisense primers sequence for the following genes (MMP1, CDK4, Caspase-3, P53, BAX, Caspase-9, Bcl2) using GAPDH as housekeeping gene.

Genes	Primer sequences
MMP <sub>1</sub>	F-5'-CTGGCCACAACTGCCAAATG-3' R-5'-CTGTCCCAGAACAGTACTTA-3'
CDK <sub>4</sub>	F-5'-TCCTAGAAGCCATCTCTCTGTG-3' R-5'-TACAAGTCTGGAGGCCAGTCAAT-3'
Caspase 3	F-5'-TTC ATT ATT CAG GCC TGC CGA GG-3' R-5'-TTC TGA CAG GCC ATG TCA TCC TCA-3'
P <sub>53</sub>	F-5'- CCCCTCCTGCCCTGTCTTC-3' R-5'-GCAGCGCCTCACAACTCCGTATCTTC-3'
Bax	F-5'-GTTTCA TCC AGG ATC GAG CAG-3' R-5'-CATCTT CTI CCA GAT GGT GA-3'
Caspase 9	F-5-GGCTGTCTACGGCACAGATGG-3 R-5-CTGGCTGGGGTTACTGCCAG-3
Bcl <sub>2</sub>	F-5'-CCTGTG GAT GAC TGA GTA CC-3' R-5'-GAGACA GCC AGG AGA AAT CA-3'
GAPDH	F-5'- TTCCAGGACCAAGATCCCTCCAAA-3' R-5'- TTCCAGGACCAAGATCCCTCCAAA-3'

crystallized ligands (Phenyl Tetrahydroisoquinoline Amide Complex, colchicines and sorafenib) respectively.

#### 3.4. QRT-PCR assay

In real time PCR analysis, all instructions, kits, conditions, were obviously discussed in details in our previous literature [32]. Colorectal carcinoma cell lines treated with (30.6 µg/ml) of compound 5 for 48 h then cells collected for total RNA extraction from both negative control and tested samples for reverse transcription steps. Suitable primers were used as illustrated in (Table 4). GAPDH was utilized as reference housekeeping gene. After all procedures were performed, quantitative determination was assessed by measurement of the threshold cycle values (CT) through the exponential phase of amplification. ΔCT was determined by the difference between the CT values of the (Caspase-3, caspase9, BAX, and cytochrome-c, BCL2, MMP1, CDK4, and VEGFR) and the value of threshold cycle (CT) of GAPDH gene. At the end, using the following equation to calculate the relative quantifications: 2- ΔCT/[Average of (2- ΔCT)].

#### 3.5. DNA fragmentation assay

Previously, in ordinary labs, the dry weight and optical density methods were commonly used for this purpose. This assay achieves our purpose without need for DNA extraction. Here, we further simplified other methods that include two steps of pretreatment with one-step (diphenylamine reagent pretreatment). DPA assay was considered as more sensitive due to less interference from other cellular components. Also, this protocol was broadly used in growth quantification. DPA colorimetric assay proved high reliability and sensitivity for the measurement of cell growth for DNA quantification with a detection limit to 3 µg DNA. Estimation was carried out at cellular level, where samples were pretreated firstly to completely dissolve cells and release deoxyriboses from DNA. Then precipitation and quantitation by (DPA) reagent were explained in detail according to our previously published paper [48]. DPA reaction was a very specific method to quantify the target DNA. Here, Genomic DNA was first hydrolyzed into many components using hot acidic conditions, where deoxyriboses were oxidized into (5-hydroxy-4-oxopentanals), which then complexed specifically condensed with DPA to form the final products with measured absorbance at 600 nm. Finally, the percent of fragmented genomic DNA was determined by the following equation: [% fragmented DNA = (A/W) × 100]; in which A = S + T, and W = S + T + B. The symbols A, and W refer to the optical density of the fragmented DNA at 600 nm.

#### 3.6. Eliza assay

"Eliza assay was utilized for quantitative measurements of Human Cytochrome c, Caspases-3, and VEGF-A concentrations in cell culture lysates. The instructions were followed up according to the manuscript instructions described in the following kits; ab119521 –Cytochrome c Human ELISA Kit, ELISA Kit catalog # KHO1091 (*Invitrogen*), and RayBio® Human VEGF-A ELISA Kit, Catalog #: ELH-VEGF respectively. We summarized the procedure described in the above manuscripts as instructed; all reagents, samples and standards were prepared. 100 µl of Standard or samples were added to each well and incubate 2.5 hrs at room temperature. 100 µl of prepared antibody was added to each well for 1 hr at room temperature. 100 µl of prepared Streptavidin solution was added and Incubate for 45 min. 100 µl of TMB One-Step Substrate Reagent was added into each well for 30 min at room temperature and finally 50 µl of Stop Solution to each well was added in addition, all readings were measured immediately at 450 nm. Curve fitting software was utilized to generate the standard curve. The concentrations for unknown samples and controls were recorded from the standard curve".

#### 3.7. Morphological characterization

In this assay, two techniques were utilized to investigate the morphological changes caused in colorectal cells due to exposure to IC<sub>50</sub> value of compound 5 for 48 hrs of treatment (Table 1). TEM instructions were performed accurately according to our previously published paper [49] with little modifications. TEM analysis was done after 48 h of incubation time, both control and treated HCT116 cells with 30.6 µg/ml of compound 5 were collected at room temperature using trypsin and centrifuged for 15 min at 15000 rpm. Then cell pellets were fixed in PBS with 2.5% glutaraldehyde and 1% osmium tetroxide, then dehydrated and inserted in an epoxy resin. Microtome sections was prepared and stained with toluidine blue (1x) and it was checked by camera Lica ICC50HD. Examination was done by transmission electron microscope JEOL, (JeolLtd., Tokyo, Japan), (JEM-1400 TEM) at the candidate magnification, and capturing image by CCD camera model AMT. To prepare the cells for ultra-structural analysis, samples were prepared as explained in TEM sample preparation, with minor changes. Dehydration of samples was performed using a graded ethanol series (30–50–70–90–100%) for each one, followed by hexamethyldisilazane (HDMS) treatment. The remaining instructions were followed as previously described in our literature [32].

#### 3.8. Cell cycle assay of HCT<sub>116</sub> treated with compound 5

"HCT116 cells at a density of 2 × 10<sup>5</sup> was cultured in 60 mm Petri dishes for 24 h and then treated with compound 5 (IC<sub>50</sub>) for 48 h. In this study, non-treated HCT116 cells were used as reference control. After incubation period, centrifugation of HCT116 cells was done at 1,200 rpm for 10 min at 4 °C. The cell pellet was suspended in PBS buffer and then centrifuged for another 10 min. Cells pellet were fixed with 70% cold ethanol overnight. After centrifugation, cells pellet was incubated with PI mixture for 30 min at room temperature. DNA content analysis was performed on Epics XL-MCL flow cytometer (Beckman Coulter, Miami, FL). Cells distribution was analyzed by Multicycle software (Phoenix Flow Systems, San Diego, CA).

#### 3.9. Apoptosis of HCT<sub>116</sub> treated with compound 5

"The apoptosis assay was studied using Annexin V-FITC kit catalog number (# 4830-01 K). HCT116 cell line was incubated with compound 5 (30.6 µg/ml) for 48 hrs. Cells centrifugation was done at 300 xg for 10 min at 37 °C. Cells were washed twice in PBS buffer(1X) and were collected for resuspension in the annexin V incubation reagent. Then 400 µl of binding buffer (1X) was added to samples [49]. Finally,

samples were analyzed by flow cytometry using FITC signal detector (usually FL-1) and PI staining by the phycoerythrin emission signal detector (usually FL-2)".

## Declaration of Competing Interest

The authors declare that they have no known competing financial interests or personal relationships that could have appeared to influence the work reported in this paper.

## Appendix A. Supplementary material

Supplementary data to this article can be found online at <https://doi.org/10.1016/j.bioorg.2020.104195>.

## References

- [1] A. Fadda, M. Mukhtar, H. Refat, Utility of activated nitriles in the synthesis of some new heterocyclic compounds, *Am. J. Org. Chem.* 22 (2012) 32–40, <https://doi.org/10.5923/j.ajoc.20120202.06>.
- [2] M.S.A. El-Gaby, A.A. Atalla, A.M. Gaber, K.A. Abd Al-Wahab, Studies on amino-pyrazoles: antibacterial activity of some novel pyrazolo[1,5-a]pyrimidines containing sulfonamido moieties, *Farm* 55 (2000) 596–602, [https://doi.org/10.1016/S0014-827X\(00\)00079-3](https://doi.org/10.1016/S0014-827X(00)00079-3).
- [3] M.A.M.S. El-Gaby, M.S.A. Taha, N.M. Micky, J.A. El-Sharief, Preparation of some novel 3,5-diaminopyrazole, pyrazolo[1,5-a][1,3,5]triazine and pyrazolo[1,5-a]-pyrimidine derivatives containing sulfonamido moieties as antimicrobial agents, *Acta Chim. Slov.* 49 (2002) 159–171.
- [4] M.S.A. El-Gaby, A.M. Gaber, A.A. Atalla, K.A. Abd Al-Wahab, Novel synthesis and antifungal activity of pyrrole and pyrrolo[2,3-d]pyrimidine derivatives containing sulfonamido moieties, *Farm.* 57 (2002) 613–617, [https://doi.org/10.1016/S0014-827X\(01\)01178-8](https://doi.org/10.1016/S0014-827X(01)01178-8).
- [5] C. Roifman, G. Aviv, L. Alexander, Preparation of N-benzyl-3-aryl-2-cyanoacrylamides activity for treatment of neoplastic disorders, *PCT. Int. Appl. WO Pat.* (2000) PCT. Int. Appl. WO Patent 2000, 0055, 128.
- [6] T. Maren, Relations between structure and biological activity of sulfonamides, *Annu. Rev. Pharmacol. Toxicol.* 16 (1976) 309–327 (accessed August 17, 2015).
- [7] B.V. Kendre, M.G. Landge, S.R. Bhusare, Synthesis and biological evaluation of some novel pyrazole, isoxazole, benzoxazepine, benzothiazepine and benzodiazepine derivatives bearing an aryl sulfonate moiety as antimicrobial and anti-inflammatory agents, *Arab. J. Chem.* 12 (2015) 2091–2097, <https://doi.org/10.1016/j.arabjc.2015.01.007>.
- [8] A.K. Tewari, V.P. Singh, P. Yadav, G. Gupta, A. Singh, R.K. Goel, P. Shinde, C.G. Mohan, Synthesis, biological evaluation and molecular modeling study of pyrazole derivatives as selective COX-2 inhibitors and anti-inflammatory agents, *Bioorg. Chem.* 56 (2014) 8–15, <https://doi.org/10.1016/j.bioorg.2014.05.004>.
- [9] S.N. Thore, S.V. Gupta, K.G. Baheti, Novel ethyl-5-amino-3-methylthio-1H-pyrazole-4-carboxylates: Synthesis and pharmacological activity, *J. Saudi Chem. Soc.* 20 (2016) 259–264, <https://doi.org/10.1016/j.jscs.2012.06.011>.
- [10] R.V. Ragavan, V. Vijayakumar, N.S. Kumari, Synthesis and antimicrobial activities of novel 1,5-diaryl pyrazoles, *Eur. J. Med. Chem.* 45 (2010) 1173–1180, <https://doi.org/10.1016/j.ejmech.2009.12.042>.
- [11] N.D. Argade, B.K. Kalrale, C.H. Gill, Microwave assisted improved method for the synthesis of pyrazole containing 2,4-disubstituted oxazole-5-one and their antimicrobial activity, *E-J. Chem.* 5 (2008) 120–129, <https://doi.org/10.1155/2008/265131>.
- [12] V. Pathak, H.K. Maurya, S. Sharma, K.K. Srivastava, A. Gupta, Synthesis and biological evaluation of substituted 4,6-diarylpyrimidines and 3,5-diphenyl-4,5-dihydro-1H-pyrazoles as anti-tubercular agents, *Bioorg. Med. Chem. Lett.* 24 (2014) 2892–2896, <https://doi.org/10.1016/j.bmcl.2014.04.094>.
- [13] M.J. Ahsan, V. Saini, Design and synthesis of 3-(4-aminophenyl)-5-(4-methoxyphenyl)-4,5-dihydro-1H-pyrazole-1-carboxamide/carbothioamide analogues as antitubercular agents, *Beni-Suef Univ. J. Basic Appl. Sci.* 4 (2015) 41–46, <https://doi.org/10.1016/j.bbjas.2015.02.006>.
- [14] S. Bondock, W. Fadaly, M.A. Metwally, Synthesis and antimicrobial activity of some new thiazole, thiophene and pyrazole derivatives containing benzothiazole moiety, *Eur. J. Med. Chem.* 45 (2010) 3692–3701, <https://doi.org/10.1016/j.ejmech.2010.05.018>.
- [15] M. Abdel-Aziz, G.E.D.A. Abuo-Rahma, A.A. Hassan, Synthesis of novel pyrazole derivatives and evaluation of their antidepressant and anticonvulsant activities, *Eur. J. Med. Chem.* 44 (2009) 3480–3487, <https://doi.org/10.1016/j.ejmech.2009.01.032>.
- [16] Ş.C. Pirol, B. Çalışkan, I. Durmaz, R. Atalay, E. Banoglu, Synthesis and preliminary mechanistic evaluation of 5-(p-tolyl)-1-(quinolin-2-yl)pyrazole-3-carboxylic acid amides with potent antiproliferative activity on human cancer cell lines, *Eur. J. Med. Chem.* 87 (2014) 140–149, <https://doi.org/10.1016/j.ejmech.2014.09.056>.
- [17] A.R. Ali, E.R. El-Bendary, M.A. Ghaly, I.A. Shehata, Synthesis, in vitro anticancer evaluation and in silico studies of novel imidazo[2,1-b]thiazole derivatives bearing pyrazole moieties, *Eur. J. Med. Chem.* 75 (2014) 492–500, <https://doi.org/10.1016/j.ejmech.2013.12.010>.
- [18] C.B. Sangani, J.A. Makawana, X. Zhang, S.B. Teraiya, L. Lin, H.L. Zhu, Design, synthesis and molecular modeling of pyrazole-quinoline-pyridine hybrids as a new class of antimicrobial and anticancer agents, *Eur. J. Med. Chem.* 76 (2014) 549–557, <https://doi.org/10.1016/j.ejmech.2014.01.018>.
- [19] K.M. Dawood, T.M.A. Eldebs, H.S.A. El-Zahabi, M.H. Yousef, P. Metz, Synthesis of some new pyrazole-based 1,3-thiazoles and 1,3,4-thiadiazoles as anticancer agents, *Eur. J. Med. Chem.* 70 (2013) 740–749, <https://doi.org/10.1016/j.ejmech.2013.10.042>.
- [20] M. Anzaldi, C. Macciò, M. Mazzei, M. Bertolotto, L. Ottone, F. Dallegrì, A. Balbi, Antiproliferative and proapoptotic activities of a new class of pyrazole derivatives in HL-60 Cells, *Chem. Biodivers.* 6 (2009) 1674–1687, <https://doi.org/10.1002/cbdv.200800354>.
- [21] A. El-Shafei, A.A. Fadda, A.M. Khalil, T.A.E. Ameen, F.A. Badria, Synthesis, anti-tumor evaluation, molecular modeling and quantitative structure-activity relationship (QSAR) of some novel arylazopyrazolodiazine and triazine analogs, *Bioorg. Med. Chem.* 17 (2009) 5096–5105, <https://doi.org/10.1016/j.bmc.2009.05.053>.
- [22] S. Lian, H. Su, B.X. Zhao, W.Y. Liu, L.W. Zheng, J.Y. Miao, Synthesis and discovery of pyrazole-5-carbohydrazide N-glycosides as inducer of autophagy in A549 lung cancer cells, *Bioorg. Med. Chem.* 17 (2009) 7085–7092, <https://doi.org/10.1016/j.bmc.2009.09.004>.
- [23] S. Elmore, Apoptosis: A review of programmed cell death, *Toxicol. Pathol.* 35 (2007) 495–516, <https://doi.org/10.1080/01926230701320337>.
- [24] M.F. Mohamed, M.S. Mohamed, M.M. Fathi, S.A. Shouman, I.A. Abdelhamid, Chalcones incorporated pyrazole ring inhibit proliferation, cell cycle progression, angiogenesis and induce apoptosis of MCF7 cell line, *Anticancer. Agents Med. Chem.* 14 (2014) 1282–1292.
- [25] M.F. Mohamed, M.S. Mohamed, S.A. Shouman, M.M. Fathi, I.A. Abdelhamid, Synthesis and biological evaluation of a novel series of chalcones incorporated pyrazole moiety as anticancer and antimicrobial agents, *Appl. Biochem. Biotechnol.* 168 (2012) 1153–1162, <https://doi.org/10.1007/s12010-012-9848-8>.
- [26] S.A.S. Ghozlan, M.F. Mohamed, A.G. Ahmed, S.A. Shouman, Y.M. Attia, I.A. Abdelhamid, Cytotoxic and antimicrobial evaluations of novel apoptotic and anti-angiogenic spiro cyclic 2-oxindole derivatives of 2-amino-tetrahydroquinolin-5-one, *Arch. Pharm. (Weinheim)* 348 (2015) 113–124, <https://doi.org/10.1002/ardp.201400304>.
- [27] M.F. Mohamed, H.K.A. Elhakim, A.A. Saddiq, I.A. Abdelhamid, A novel inhibitor, 2-cyano-3-(1-phenyl-3-(thiophen-2-yl)-pyrazol-4-yl)acrylamide linked to sulphamethoxazole, blocks anti-apoptotic proteins via molecular docking and strongly induced apoptosis of HCT116 cell line by different molecular tools, *Arab. J. Chem.* 13 (2020) 5978–5995, <https://doi.org/10.1016/j.arabjc.2020.04.032>.
- [28] A.M. Abdelmoniem, M.F. Mohamed, D.M. Abdelmoniem, S.A.S. Ghozlan, I.A. Abdelhamid, Recent synthetic approaches and biological evaluations of amino hexahydroquinolines and their spirocyclic structures, *Anticancer. Agents Med. Chem.* 19 (2019) 875–915, <https://doi.org/10.2174/1871520619666190131140436>.
- [29] N.Y. Gorobets, B.H. Yousefi, F. Belaj, C.O. Kappe, Rapid microwave-assisted solution phase synthesis of substituted 2-pyridone libraries, *Tetrahedron* 60 (2004) 8633–8644, <https://doi.org/10.1016/j.tet.2004.05.100>.
- [30] J. Štětinová, R. Kada, J. Lesko, M. Dandarová, M. Krublová, Synthesis and spectral properties of 1-(6-methoxy-2-benzothiazolyl)-2-pyridones, *Collect. Czech. Chem. Commun.* 61 (1996) 921–929.
- [31] M.F. Mohamed, Y.M. Attia, S.A. Shouman, I.A. Abdelhamid, Anticancer activities of new N-hetaryl-2-cyanoacetamide derivatives incorporating 4,5,6,7-tetrahydrobenzo[b]thiophene moiety, *Anticancer. Agents Med. Chem.* 17 (2017) 1084–1092, <https://doi.org/10.2174/1871520617666170110154110>.
- [32] M.F. Mohamed, N. Samir, A. Ali, N. Ahmed, Y. Ali, S. Aref, O. Hossam, M.S. Mohamed, A.M. Abdelmoniem, I. Abdelhamid, Apoptotic induction mediated p53 mechanism and Caspase-3 activity by novel promising cyanoacrylamide derivatives in breast carcinoma, *Bioorg. Chem.* 73 (2017) 43–52, <https://doi.org/10.1016/j.bioorg.2017.05.012>.
- [33] K. Barton, Determination of DNA concentration with diphenylamine, *Methods Enzym.* 50 (1968) 349–383.
- [34] F.M. Ranaivoson, B. Gigant, S. Berritt, M. Joullié, M. Knossow, IUCr, Structural plasticity of tubulin assembly probed by vinca-domain ligands, *Acta Crystallogr. Sect. D Biol. Crystallogr.* 68 (2012) 927–934, <https://doi.org/10.1107/S0907444912017143>.
- [35] K. Okamoto, M. Ikemori-Kawada, A. Jestel, K. von König, Y. Funahashi, T. Matsushima, A. Tsuruoka, A. Inoue, J. Matsui, Distinct binding mode of multi-kinase inhibitor lenvatinib revealed by biochemical characterization, *ACS Med. Chem. Lett.* 6 (2015) 89–94, <https://doi.org/10.1021/ml500394m>.
- [36] J. Porter, A. Payne, B. de Candole, D. Ford, B. Hutchinson, G. Trevitt, J. Turner, C. Edwards, C. Watkins, J. Whitcombe, J. Davis, C. Stubberfield, Tetrahydroisoquinoline amide substituted phenyl pyrazoles as selective Bcl-2 inhibitors, *Bioorg. Med. Chem. Lett.* 19 (2009) 230–233, <https://doi.org/10.1016/j.bmcl.2008.10.113>.
- [37] I.R. Indran, G. Tufo, S. Pervaiz, C. Brenner, Recent advances in apoptosis, mitochondria and drug resistance in cancer cells, *Biochim. Biophys. Acta - Bioenerg.* 2011 (1807) 735–745, <https://doi.org/10.1016/j.bbabi.2011.03.010>.
- [38] K.I. Block, C. Gyllenhaal, L. Lowe, A. Amedei, A.R.M. Ruhul Amin, A. Amin, K. Aquilano, J. Arbiser, A. Arreola, A. Arzumanyan, S. Salman Ashraf, A.S. Azmi, F. Benencia, D. Bhakta, A. Bilsland, A. Bishayee, S.W. Blain, P.B. Block, C.S. Boosani, T.E. Carey, A. Carnero, M. Carotenuto, S.C. Casey, M. Chakrabarti, R. Chaturvedi, G.Z. Chen, H. Chen, S. Chen, Y.C. Chen, B.K. Choi, M.R. Ciriolo, H.M. Coley, A.R. Collins, M. Connell, S. Crawford, C.S. Curran, C. Dabrosin, G. Damia, S. Dasgupta, R.J. DeBerardinis, W.K. Decker, P. Dhawan, A.M.E. Diehl,

- J.T. Dong, Q.P. Dou, J.E. Drewa, E. Elkord, B. El-Rayes, M.A. Feitelson, D.W. Felsheru, L.R. Ferguson, C. Fimognari, G.L. Firestone, C. Frezza, H. Fujii, M.M. Fuster, D. Generali, A.G. Georgakilas, F. Gieseler, M. Gilbertson, M.F. Green, B. Grue, G. Guhal, D. Halicka, W.G. Helferich, P. Heneberg, P. Hentosh, M.D. Hirschev, L.J. Hofseth, R.F. Holcombe, K. Honoki, H.Y. Hsu, G.S. Huang, L.D. Jensen, W.G. Jiang, L.W. Jones, P.A. Karpowicz, W.N. Keith, S.P. Kerkar, G.N. Khan, M. Khatami, Y.H. Ko, O. Kucuk, R.J. Kulathinal, N.B. Kumar, B.S. Kwon, A. Leb, M.A. Leab, H.Y. Lee, T. Lichtor, L.T. Lin, J.W. Locasale, B.L. Lokeshwar, V.D. Longo, C.A. Lyssiotis, K.L. MacKenzie, M. Malhotra, M. Marino, M.L. Martinez-Chantar, A. Matheu, C. Maxwell, E. McDonnell, A.K. Meeker, M. Mehrmohamadi, K. Mehta, G.A. Michelotti, R.M. Mohammad, S.I. Mohammed, D.J. Morre, I. Muqbil, V. Muralidharcq, M.P. Murphy, G.P. Nagaraju, R. Nahta, E. Niccolai, S. Nowsheen, C. Panis, F. Pantano, V.R. Parslow, G. Pawelec, P.L. Pedersen, B. Poore, D. Poudyal, S. Prakash, M. Prince, L. Raffaghello, J.C. Rathmell, W.K. Rathmell, S.K. Ray, J. Reichrath, S. Rezazadeh, D. Ribatti, L. Ricciardiello, R.B. Robeydf, F. Rodierdh, H.P.V. Rupasinghe, G.L. Russo, E.P. Ryan, A.K. Samadi, I. Sanchez-Garcia, A.J. Sanders, D. Santini, M. Sarkar, T. Sasada, N.K. Saxena, R.E. Shackelford, H.M.C. Shantha Kumara, D. Sharma, D.M. Shin, D. Sidransky, M.D. Siegelin, E. Signori, N. Singh, S. Sivanand, D. Sliva, C. Smythe, C. Spagnuolo, D.M. Stafforini, J. Stagg, P.R. Subbarayan, T. Sundin, W.H. Talib, S.K. Thompson, P.T. Tran, H. Ungefroren, M.G. Vander Heiden, V. Venkateswaran, D.S. Vinay, P.J. Vlachostergios, Z. Wang, K.E. Wellen, R.L. Whelan, E.S. Yang, H. Yang, X. Yang, P. Yaswen, C. Yedjou, X. Yin, J. Zhu, M. Zollo, Designing a broad-spectrum integrative approach for cancer prevention and treatment, *Semin. Cancer Biol.* 35 (2015) S276–S304, <https://doi.org/10.1016/j.semcan.2015.09.007>.
- [39] Y. Zhao, S. Xiang, X. Dai, K. Yang, A simplified diphenylamine colorimetric method for growth quantification, *Appl. Microbiol. Biotechnol.* 97 (2013) 5069–5077, <https://doi.org/10.1007/s00253-013-4893-y>.
- [40] K. Burton, A study of the conditions and mechanism of the diphenylamine reaction for the colorimetric estimation of deoxyribonucleic acid, *Biochem. J.* 62 (1956) 315–323, <https://doi.org/10.1042/bj0620315>.
- [41] F.A. Sinicrope, R.L. Rego, K. Okumura, N.R. Foster, M.J. O'Connell, D.J. Sargent, H.E. Windschitl, Prognostic impact of Bim, Puma, and Noxa expression in human colon carcinomas, *Clin. Cancer Res.* 14 (2008) 5810–5818, <https://doi.org/10.1158/1078-0432.CCR-07-5202>.
- [42] D. Green, G. Kroemer, The central executioners of apoptosis: Caspases or mitochondria? *Trends Cell Biol.* 8 (1998) 267–271, [https://doi.org/10.1016/S0962-8924\(98\)01273-2](https://doi.org/10.1016/S0962-8924(98)01273-2).
- [43] S. Fulda, L. Galluzzi, G. Kroemer, Targeting mitochondria for cancer therapy, *Nat. Rev. Drug Discov.* 9 (2010) 447–464, <https://doi.org/10.1038/nrd3137>.
- [44] S.F. Martins, E.A. Garcia, M.A.M. Luz, F. Pardal, M. Rodrigues, A.L. Filho, Clinicopathological correlation and prognostic significance of VEGF-A, VEGF-C, VEGFR-2 and VEGFR-3 expression in Colorectal cancer, *Cancer Genomics Proteomics* 10 (2013) 55–68.
- [45] V. Perumal, S. Banerjee, S. Das, R.K. Sen, M. Mandal, Effect of liposomal celecoxib on proliferation of colon cancer cell and inhibition of DMBA-induced tumor in rat model, *Cancer Nanotechnol.* 2 (2011) 67–79, <https://doi.org/10.1007/s12645-011-0017-5>.
- [46] R.H. Medema, L. Macurek, Checkpoint control and cancer, *Oncogene* 31 (2012) 2601–2613, <https://doi.org/10.1038/onc.2011.451>.
- [47] M.F. Mohamed, H.M. Hassaneen, I.A. Abdelhamid, Cytotoxicity, molecular modeling, cell cycle arrest, and apoptotic induction induced by novel tetrahydro-[1,2,4] triazolo[3,4-a]isoquinoline chalcones, *Eur. J. Med. Chem.* 143 (2018) 532–541, <https://doi.org/10.1016/J.EJMECH.2017.11.045>.
- [48] M.A. Tantawy, F.M. Sroor, M.F. Mohamed, M.E. El-Naggar, F.M. Saleh, H.M. Hassaneen, I.A. Abdelhamid, Molecular docking study, cytotoxicity, cell cycle arrest and apoptotic induction of novel chalcones incorporating thiadiazolyl isoquinoline in cervical cancer, *Anticancer. Agents Med. Chem.* 19 (2019), <https://doi.org/10.2174/1871520619666191024121>. doi:10.2174/1871520619666191024121116.
- [49] A.G. Ali, M.F. Mohamed, A.O. Abdelhamid, M.S. Mohamed, A novel adamantane thiadiazole derivative induces mitochondria-mediated apoptosis in lung carcinoma cell line, *Bioorg. Med. Chem.* 25 (2017) 241–253, <https://doi.org/10.1016/j.bmc.2016.10.040>.